REGISTERED No. M. 3121

UNIVERSITY OF MICHIGAN
OCT 13 1954
PHYSICS LIBRARY

PROCEEDINGS
OF THE
INDIAN ACADEMY
OF SCIENCES

VOL. XL] *SECTION A* [No. 2

AUGUST 1954

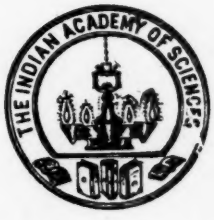

Price Rs. 2 or 3 Sh. *Annual Subscription Rs. 18*

PRINTED AT THE BANGALORE PRESS, BANGALORE CITY, BY C. VASUDEVA RAO, SUPERINTENDENT AND PUBLISHED BY THE INDIAN ACADEMY OF SCIENCES, BANGALORE.

X-RAY STUDIES ON POLYCRYSTALLINE GYPSUM

By Sir C. V. Raman and A. Jayaraman
(*Memoir No. 56, from the Raman Research Institute, Bangalore*)

Received August 16, 1954

1. Introduction

Gypsum is one of the most important of the commoner minerals and the different forms in which it is found and their structural characters are therefore matters of considerable interest. Brauns' *Das Mineralreich*[1] and Hintze's *Handbuch der Mineralogie*[2] contain illustrated accounts of the subject. We are concerned in this paper with the polycrystalline forms of gypsum. Of these the best known is the white and semi-opaque material known as alabaster. Mineralogists recognise another form which they designate as "fibrous gypsum". As the name indicates, this form is an aggregate of parallel fibres or rods. Hintze mentions that when the fibres in such gypsum are very fine, their direction is parallel to the mineralogical *c*-axis, while if the material consists of coarser fibres, their direction may depart to a greater or less extent therefrom.

In a recent paper in these *Proceedings*,[3] it has been shown that we must recognize *three* polycrystalline forms of gypsum with specific characters which are readily distinguishable from each other. The first is *alabaster* which is an aggregate of small crystals more or less randomly orientated: the second is *satin-spar* which is a truly fibrous variety of gypsum in which the fibres lie along the mineralogical *c*-axis, while the third form has been designated as *fascicular gypsum* and is an aggregate of rods more or less exactly parallel to the *b*-axis which is also the symmetry axis of the crystal-structure. This third form is readily distinguished from the other two by its external appearance. It exhibits optical phenomena of great beauty and interest which have been fully described and explained in the paper referred to above. In the present communication, we report the results of X-ray studies undertaken to confirm and reinforce the conclusions already reached in that paper from the optical evidence. We have thought it desirable to carry out such an investigation for the reason that the third form of gypsum is of common occurrence and it would seem that those who have noticed it have mistaken it for the second or fibrous species. Our X-ray studies show clearly that the direction of the rods in fascicular gypsum is along the *b*-axis, while in the truly fibrous forms it is along the *c*-axis. Further,

while the X-ray patterns show that satin-spar gives a typical fibre diagram, fascicular gypsum does not do so, showing thereby that it is not fibrous in the proper sense of the word.

2. ALABASTER

This polycrystalline form of gypsum varies greatly in its appearance in different specimens, some being chalky-white and opaque even in thin layers, while other specimens appear translucent. These differences are evidently connected with the extent to which light can penetrate through the material and this again appears to depend on the size of the crystallites of which it is composed. Selecting a translucent specimen of alabaster and thinning it down to a plate about a millimetre thick, the X-ray diffraction diagram reproduced as Fig. 1 in Plate III was recorded. A collimated beam of MOK_α radiation was employed. The slit width was one millimetre and a flat film camera was used with a specimen to film distance of three centimetres. It will be seen that the diagram exhibits spotty rings. Though the pattern is not altogether symmetric, it is sufficiently nearly so to justify our regarding the material as consisting of crystallites randomly orientated in space.

3. SATIN-SPAR

The specimens employed were detached from the surface of a beautiful museum piece which externally manifests a fibrous and brilliant silky lustre. Figure 2 in Plate III is an X-ray diagram taken with a flat camera and unfiltered MO radiation: the incident beam travelled along the fibre direction. The specimen employed was about a millimetre in length and of about the same cross-section. It will be seen that the pattern exhibits numerous and nearly complete concentric circular rings.

Figure 4 in Plate IV was recorded with a cylindrical camera and CuK_α radiation. The specimen in this case was a rod about one centimetre long and about half a millimetre in thickness. It was held inside the camera with its length parallel to the axis of the cylinder and the X-ray beam traversed the specimen in a direction perpendicular to its length. The specimen was kept stationary during the exposure. Nevertheless it will be seen that the pattern is a typical rotation diagram. It was verified by measurement of the separation of the layer lines that the length of the fibre was parallel to the mineralogical *c*-axis of gypsum. The conclusion thus indicated that satin-spar is a truly fibrous material orientated along the morphological *c*-axis is, however, only valid for the material used which was detached from the external surface of the museum specimen. When a thin plate cut from the latter with its faces transverse to the fibre direction was normally irradiated

by an X-ray beam in a flat-film camera, the record appeared both spotty and irregular, thus indicating a departure from the regularity of orientation shown by the material detached from its outer surface.

4. Fascicular Gypsum

As already stated, this material exhibits highly characteristic external features which enable it to be readily identified. It may be readily split into slabs or sheets of any thickness, but the surfaces thus exposed do not exhibit the smoothness and optical perfection characteristic of the cleavage of selenite and are more appropriately described as planes of parting. The most distinctive feature of the mineral is that the edges of the blocks or slabs are not smooth but exhibit parallel ridges. The inference suggested by the external appearance of the material is that it is an aggregate of rods in parallel setting, their direction coinciding approximately with the *b* or the symmetry axis of gypsum.

Figure 5 in Plate IV is an X-ray pattern recorded with cylindrical camera and CuK_α radiation. The specimen examined was a rod detached from the material and set with its length parallel to the axis of the camera. It was kept stationary during the exposure. The pattern exhibits irregularly disposed spots. The configuration of the latter indicated that the length of the rod was not quite parallel to the *b*-axis, but was slightly inclined to the latter. The rod was turned through $3\frac{1}{2}°$ from the previous position, but nevertheless the pattern then obtained did not exhibit the characteristic features of a rotation diagram. However, when the specimen was oscillated through 30° each way, a record was obtained which is reproduced in Fig. 6 in Plate IV and clearly exhibits layer lines. These are much closer to each other than those appearing in Fig. 4 in the same Plate. Measurements indicated that the oscillation axis coincided with the *b* or symmetry axis of gypsum.

Figure 3 in Plate III shows an X-ray diagram obtained with a flat film camera and the MO radiation, the beam being parallel to the length of the rods. It will be seen from the pattern that the X-ray reflections recorded appear as patches located roughly on short arcs of circles. The picture indicates that while the rods consist of individual crystals having their *b*-axes parallel, the variations of orientation of the other two crystallographic axes are insufficient in magnitude to give a complete pattern of circular rings. The inferences regarding the nature of the material indicated both by the longitudinal and transverse X-ray photographs thus support each other. The X-ray results are also in agreement with the conclusions already drawn from the optical investigations and described in the earlier paper.

5. SUMMARY

X-ray diffraction patterns have been recorded and are reproduced in the paper showing clearly the existence of *three* polycrystalline forms of gypsum with specific structural characters which are readily distinguishable from each other: (*a*) alabaster; (*b*) satin-spar, which is a truly fibrous material with the fibres orientated along the mineralogical *c*-axis; and (*c*) fascicular gypsum which is an aggregate of rods having their *b*-axes or crystallographic symmetry axes parallel to each other and the two other axes showing only a limited range of variation, and hence not fibrous in the proper sense of the word.

6. REFERENCES

1. Brauns, R. .. *Das Mineralreich*, J. F. Schreiber, 1912, 408–14.
2. Hintze, Carl .. *Handbuch der Mineralogie*, Erster Band. Dritte Abteilung, Zweite Halfte, Walter De Gruyter & Co., 1930, 4274–4323.
3. Raman, C. V. and Ramdas, A. K. *Proc. Ind. Acad. Sci.*, 1954, **39A**, 153–61.

FIG. 1

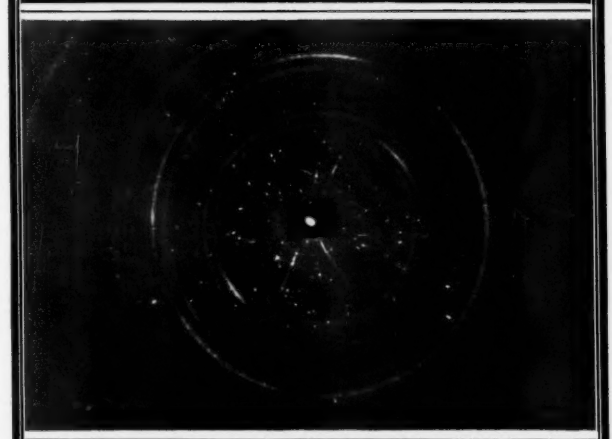

FIG. 2

FIG. 3

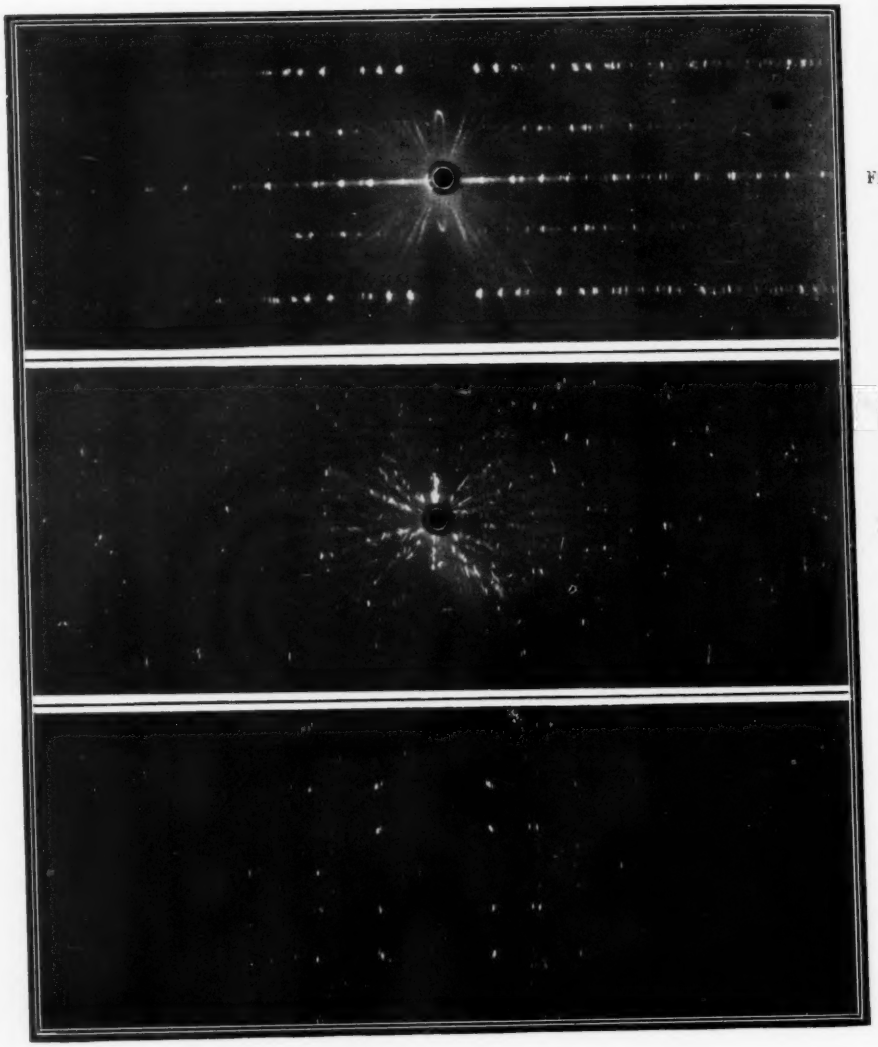

FIG. 4

FIG. 5

FIG. 6

ANGULAR DISTRIBUTION OF PROTONS EMITTED IN THE REACTION $_7N^{14}(\alpha, p)_8O^{17}$

By G. S. Mani and R. Pandhi

(Tata Institute of Fundamental Research, Bombay)

Received June 10, 1954

(Communicated by Dr. H. J. Bhabha)

Using a conventional six-inch Wilson Chamber with a special collimating system for the alpha particles, 353 useful proton tracks emitted in the reaction $_7N^{14}(\alpha, p)_8O^{17}$ have been obtained in a total of 8,000 pictures. The source of alpha particles was a 10 mc. polonium source electrolytically deposited on a 2×2 mm. platinum foil. The collimating system consisted of a rectangular brass frame with two parallel thin gold foils soldered to its sides (Fig. 1). The thickness of the gold foil was enough to stop the alpha particles but allow the protons from the $_7N^{14}(\alpha, p)_8O^{17}$ reaction to enter the sensitive volume of the chamber. The source was kept at one end of the frame and the alpha particles were allowed to enter into the region between the gold foils through a small hole 1·5 mm. in diameter. The advantages of such a system are: (1) The source is isolated from the sensitive volume of the chamber and as such prevents the spread of the alpha contamination into the chamber. (2) Throughout the range of the alpha beam the lateral spread is restricted to 2 mm. (3) Only 0·2 mm. of the alpha range is lost in the process of collimation. (4) The amount of target gas required is small as it needs to be introduced only into the small region between the gold foils. The only difficulty of the method is that the thin gold foils occasionally get punctured and introduce gas motion inside the chamber. The tracks were photographed by two cameras whose axes were inclined to each other at 30°, one of the cameras being mounted normal to the plane of the chamber.

It can be shown that, if $R_\alpha{}^x$ and $R_\alpha{}^y$ be the projected ranges of the alpha particles in the cameras and $\phi_p{}^x$ and $\phi_p{}^y$ be the projected angles that the emergent proton makes with the direction of the alpha particles, then the actual range R_α and angle ϕ_ρ is given by

$$R_\alpha = (R_\alpha{}^x + R_\alpha{}^y)\,[\cos\theta + \sin(\gamma + \theta)]^{-1}$$

$$\cos\phi_p = \frac{1}{\sqrt{\Delta}}\,[\sin\theta \sin\phi_p{}^x \cos\phi_p{}^y - \cos\phi_p{}^x \sin\phi_p{}^y \sin\gamma]^2$$

$$\Delta = \sin^2\phi_p{}^y \cos^2\gamma + [\sin\phi_p{}^x \cos\phi_p{}^y - \cos\phi_p{}^x \sin\phi_p{}^y \sin\gamma]^2$$

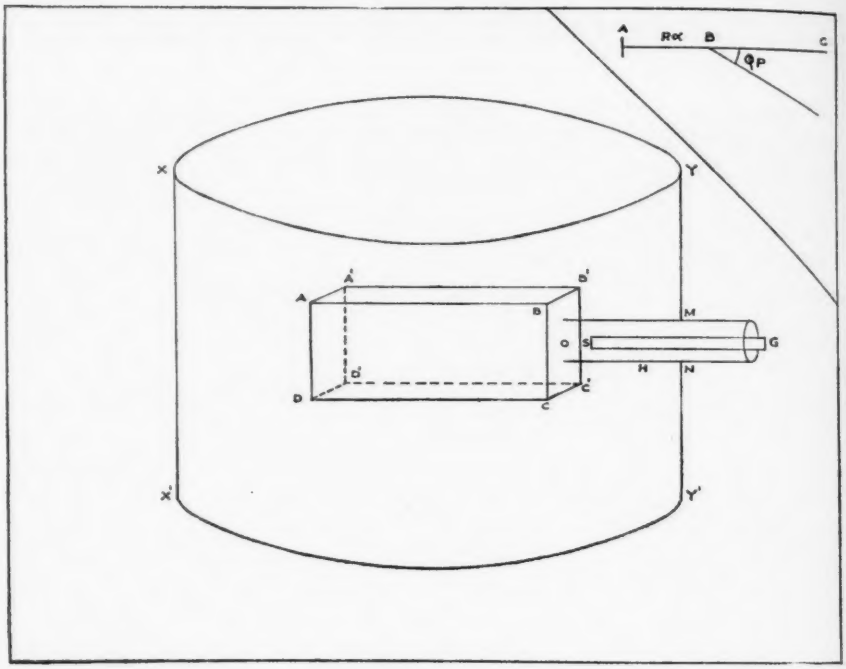

FIG. 1

Inset: ABCD represents the tracks as they appear in the cameras, AB being the length of alpha particle before causing the reaction.

$(90° - \gamma)$ being the angle that the axis of the inclined camera makes with the vertical. If θ be the angle made by the alpha particle that causes the reaction with the axis of the alpha beam then we further have

$$\tan \theta = \frac{R_a{}^y - R_a{}^x \sin \gamma}{R_a{}^x \cos \gamma}.$$

The following resonance levels of the compound nucleus $_9F^{18}$ were obtained: 2 Mev, 3·6 Mev. and 4·1 Mev which agree well with the previous work on this subject.[1, 2, 3, 4]

The criteria for selection of proton tracks were: (1) tracks less than 0·5 cm. were rejected and (2) tracks not visibly originating in the alpha beam were rejected. Corrections for the geometry of the target chamber, illumination and loss of protons due to the restrictions on the selection of tracks were made to the angular distribution curves. If I (β) be the number of particles

in the C.M. system for the C.M. angle β, and $I(\phi)$ the number of particles found experimentally for the corresponding lab angle ϕ, then

$$I(\beta) = I(\phi)\, \rho\, \delta$$

ρ being the correction due to the above reasons, and δ the factor for transformation from lab to C.M. system.[5] The following integral which was obtained for ρ was evaluated graphically.

$$\rho = \frac{\int_0^{\theta_{max}} N'(\theta)\, d\theta}{\int_0^{\alpha} N'(\theta)\, d\theta + \int_{\alpha}^{\beta} kN'(\theta)\, d\theta}$$

where

$$N'(\theta) = 2tl \frac{\operatorname{cosec}\theta\,(\operatorname{cosec}^2\theta + \cot^2\theta)}{\cot^2\theta\,(l^2\operatorname{cosec}^2\theta + t^2) + t^2}$$

$$k = 1 - \frac{1}{\pi}\left[\frac{l_1 - R\sin\theta - l_p\cos\phi\sin\theta}{l_p\sin\phi\cos\theta}\right]$$

$$\alpha = |\theta|_{k=1} \qquad \text{for } \phi < (\pi - \theta_1)$$

$$= \theta_1 \qquad \text{for } \phi \geqslant (\pi - \theta_1)$$

$$\beta = |\theta|_{k=0} \qquad \text{for } \phi < \theta_1$$

$$= \theta_1 \qquad \text{for } \phi \geqslant \theta_1$$

$$\theta_1 = \sin^{-1} l_1/R.$$

R being the range of the alpha particle, l being the total height of the target chamber, t the thickness of the target chamber, $2l_1$ the total height of the illuminated region, and l_p the minimum length of proton track that was accepted. The angular distribution for the 4·1 and 3·6 Mev levels was given by (see Figs. 2 and 3)

$$I(\beta) = (1 - 1{\cdot}1\cos^2\beta)$$

for both the levels, in agreement with previous work.

The 2 Mev level shows a maximum at about 115° and the distribution was found to be (see Fig. 4)

$$I(\beta) = (1 - {\cdot}64\cos\beta - 1{\cdot}2\cos^2\beta)$$

using the usual method of least squares. χ^2 test yielded a fit of 60%. This distribution is in disagreement with that obtained by Roy and Champion.[2]

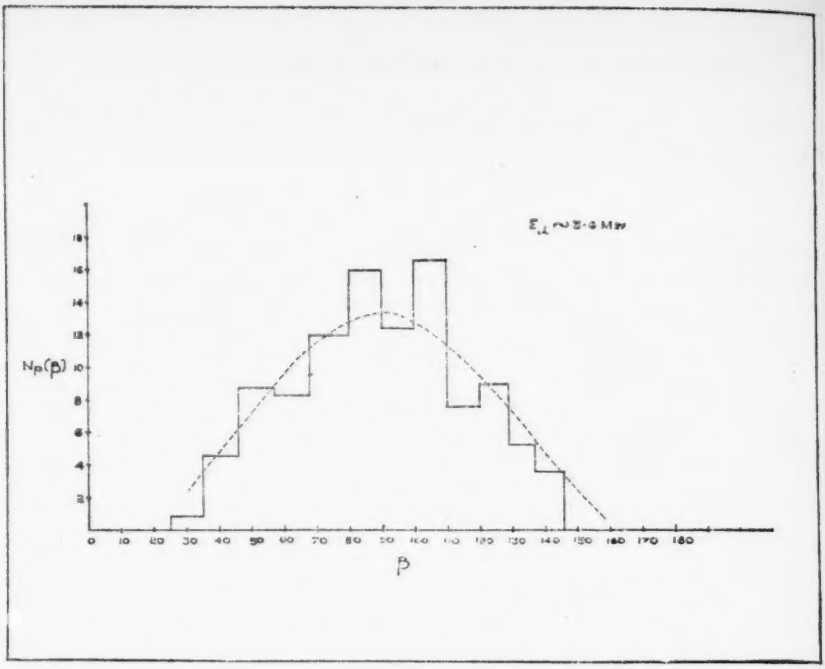

FIG. 2

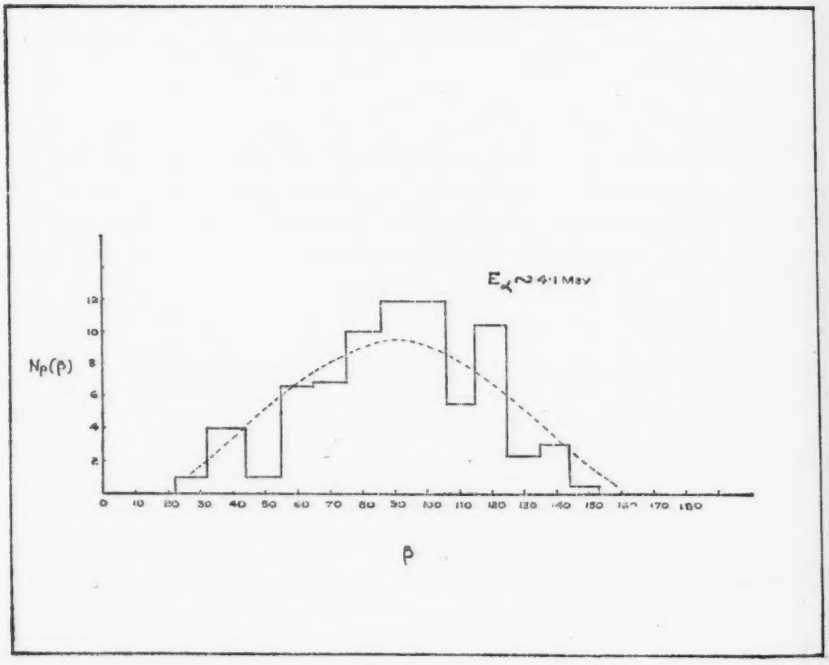

FIG. 3

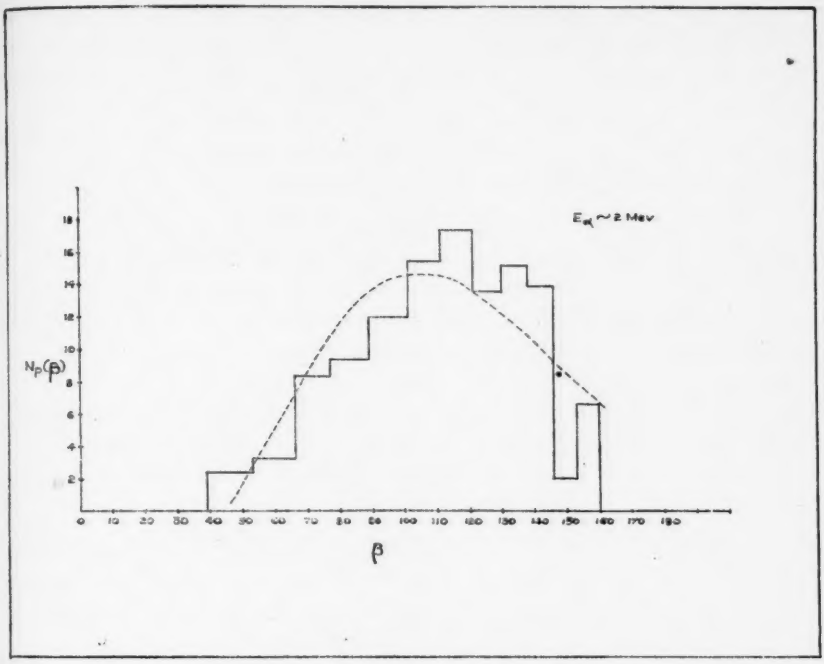

FIG. 4

The odd neutron and odd proton in $_7N^{14}$ are in the $p_{\frac{1}{2}}$ state yielding a total spin 1 and even parity. The odd neutron of $_8O^{17}$ is in the $d_{5/2}$ state leading to spin 5/2 and even parity. Hence the emitted proton will have the same parity as the incident alpha particle. Yang[6] has proved on general grounds the following theorem: . When contributions from incoming waves of orbital angular momenta greater than L are neglected, the angular distribution in the C.M. system is an even polynomial of cos β with maximum exponent not greater than 2L. Any odd power of cos β occurring in the angular distribution is due to interference between orbital wave functions of opposite parity. Hence the 3·6 and 4·1 Mev levels are mainly excited by P waves. Roy (1950) observed that the excited state of O^{17} yields an isotropic distribution indicating the existence of an S wave. Since our 2 Mev level has a dominant coefficient in $\cos^2 \beta$ and a small one in cos β, we conclude that it is chiefly caused by the P wave together with an admixture of S wave and that the compound nuclear level corresponding to this energy is a mixture of at least two levels of opposite parity.

Our thanks are due to Dr. R. Ramanna who suggested this problem and guided us throughout the course of this work. Also we would like to express our thanks to Mr. P. N. Rama Rao for his assistance in wiring the necessary electronic circuits.

REFERENCES

1. Stegmann .. *Z. Phys.*, 1935, **95**, 72.
2. Champion and Roy .. *Proc. Roy. Soc.*, 1947, **191**, 269.
3. R. R. Roy .. *Bulletin Centre de Phys. Nucleaire*, Univ. Libre de Bruxelles, September 1950, No. **21**.
4. ———— .. *Phys. Rev.*, 1951, **82**, 227.
5. Mandeville .. *J. Frank. Inst.*, 1947, **244**, 385.
6. Yang .. *Phys. Rev.*, 1948, **74**, 764.

AN X-RAY STUDY OF NATURAL MONAZITE: I

By M. D. Karkhanavala and J. Shankar

(Chemistry Division, Atomic Energy Commission, Bombay)

Received November 30, 1953

(Communicated by Prof. H. J. Bhabha)

I. Introduction

In the course of the present investigation of the structure of monazite by X-rays, it was observed that samples from different localities all gave very diffuse powder diffraction patterns even after fairly long exposures, a fact indicating the possible existence of monazite in the metamict state. Such an occurrence would not be surprising in view of the high thorium content of the mineral but for the fact that monazite is commonly considered to be nonmetamict (Hutton, 1950; Hurley and Fairben, 1953). It was therefore decided to carefully investigate this possibility.

II. Review of Literature

Very few X-ray studies on monazite are reported in the literature, and almost all of them are single crystal studies. The only known powder diffraction data is the partial one recently published by Pabst (1951) and reproduced in the ASTM Hanawalt Card Index (4th set, Card No. 4–0612).

The earliest results of an X-ray study of a monazite crystal were reported by Ramdohr (1936) in Klochmann's *Lehrbuch der Mineralogie:*

$$a = 6{\cdot}78 \qquad b = 6{\cdot}99 \qquad c = 6{\cdot}45\ \text{Å} \qquad \beta = 76^\circ\ 20'$$

$$Z = 4;\ \text{space group}\ C^5_{2h}$$

Later Gliszczynski (1939) studied the rotation and oscillation photographs of a single crystal of Turnerite from Perdatsh, Switzerland. The cell constants so determined substantiated the earlier values. The β-angle was found to be 76° 22′.

Independently Parrish (1939) determined the cell constants of a spectroscopically thorium-free single crystal of monazite from Llallagua, Bolivia, using the equi-inclination Weissenberg method. The values agreed well with those reported earlier, the only major difference being the β-angle which according to him was 76° 50′.

Pabst (1951) has given a few other references to the X-ray analysis of monazite but these were not accessible to the authors.

The chemical analysis or the thorium content, if any, of the monazite crystals used were not reported by any of these authors except Parrish. On

the basis of these reported results it is difficult to say, whether thorium containing monazite is metamict or not.

It is worthwhile nevertheless to note the following in Gliszczynski's paper. As stated above he has not reported the chemical analysis of the crystals used, which are merely referred to as $CePO_4$. However, while discussing the powder photographs of monasite from Brazil and of the turnerite from Perdatsh, he has apoligised for the poor quality of the photographic reproduction of the two patterns. The monazite pattern (his Fig. 2) is very indistinct while that of turnerite (his Fig. 3) is comparatively sharper though still indistinct. It is also important to note that the density of the single crystal of turnerite referred to by him as $CePO_4$ was 5·217 g. cm.$^{-3}$ Parrish has reported that the density of the chemically analysed thorium-free crystal of monazite used was 5·173 g. cm.$^{-3}$ while the density calculated by him on the basis of 4 molecules of $(La_{4/9}, Ce_{4/9}, Y_{1/9})PO_4$ per unit cell was 5·06 g. cm.$^{-3}$ It is very likely, therefore, that the crystals examined by Gliszczynski contained significant amounts of thorium. It is not intended, however, to make a case for the metamictness of the samples used by Gliszczynski, but only to point out what might possibly have been the first reported case of a metamict monazite.

III. EXPERIMENTAL

The locality, the physical state, and the thorium oxide content of the samples used are given in Table I.

TABLE I. *ThO_2 Content of Monazite Samples*

Sample No.	Locality	Physical State	ThO_2%
1	India	Massive	15
2	India	Massive	7·5
3	Brazil	Massive	6
4	India	Sand (handpicked)	9

The samples were ground to less than 250 mesh and the Debye-Scherrer powder patterns were obtained in a 114·6 mm. diameter camera on a GE-XRD 3 machine using filtered CuK_α radiation at 35 KV and 20 MA. All the samples were exposed for a period of 4·75 hours and the films developed for 3·5 minutes at 75° F. A representative pattern is shown in Fig. 1 (*a*).

The samples were then individually heated in a platinum boat to 1130° C., maintained at that temperature for 24 hours in a " globar " electric furnace and air quenched. This temperature was chosen as the most suitable from

the results of the preliminary heating runs carried out at different temperatures. Debye-Scherrer powder patterns of the heat-treated samples were obtained under conditions identical with those stated above, except that the exposure time was reduced to 3 hours. The developing time and the temperature were not altered. The corresponding pattern after heat treatment is shown in Fig. 1 (*b*). Since the only available powder diffraction data [Pabst (1951)] on monazite is not complete, it is thought desirable to complete this data. The *d*-spacings of one of the heat-treated samples are therefore given in Table II. Indices were assigned assuming the unit cell dimensions and the space group reported by Gliszczynski.

TABLE II. *Powder Diffraction Data for Heat Treated Monazite*

(Filtered CuKα Radiation, $r = 114{\cdot}6$ mm.)

I/I_0	$d_{cal.}$ (A.U.)	$d_{obs.}$ (A.U.)	*hkl*
W	5·193	5·18	101
W	4·665	4·65	011
M	4·169	4·16	$\bar{1}11$
VW	4·085	4·10	$\bar{1}01$
M	3·496	3·50	020
S	3·296	3·28	200
VS	3·089	3·09	120
W	2·980	2·97	210
VS	2·856 2·857	2·86	012 112
M	2·597	2·60	202
W	2·493	2·52	$\bar{2}11$
M	2·438	2·44	$\bar{1}12$
VW	2·398	2·40	220
VVW	2·334 2·331	2·34	022 122
VVW	2·247	2·25	301
M	2·185	2·19	031
S	2·141 2·138	2 14	103 311
VVW	2·087 2·084	2·07	$\bar{1}22$ 222
VW	2·047	2·02	113
W	2·001	2·00	013
S	1·961	1·97	$\bar{2}12$
VW	1·957	1·95	312
M	1·912	1·90	213
S	1·870 1·868	1·87	032 $\bar{1}03$
VVW	1·827	1·83	123
VW	1·804	1·81	$\bar{1}13$
M	1·763 1·761	1·77	$\bar{2}22$ 322
S	1·748	1·75	040
M	1·731 1·728	1·72	303 223
W	1·693	1·71	$\bar{3}21$
M	1·680	1·67	313
W	1·648 1·648 1·647	1·65	400 411 $\bar{1}23$
W	1·624	1·63	402
M	1·604	1·61	410
VW	1·588	1·59	004
M	1·539	1·54	033
M	1·508	1·49	124
M	1·475 1·475 1·473	1·47	$\bar{3}22$ $\bar{4}11$ 422
W	1·455	1·46	$\bar{2}23$

TABLE II (*Continued*)

I/I_0	$d_{cal.}$ (A.U.)	$d_{obs.}$ (A.U.)	*hkl*
VVW	1·445	1·44	042
	1·442		413
VVW	1·422	1·43	$\bar{1}14$
VW	1·3897	1·39	333
VW	1·384	1·38	$\bar{4}21$
M	1·368	1·37	150
	1·365		051
W	1·362	1·36	$\bar{3}03$
	1·358		423
MS	1·337	1·34	324
MS	1·334	1·33	$\bar{4}02$
	1·331		511
VW	1·311	1·31	$\bar{4}12$
	1·308		340
	1·301		$\bar{2}04$
VW	1·300	1·30	034
	1·298		404
	1·284		414
MS	1·277	1·28	043
	1·277		052
VW	1·264	1·26	521
	1·256		503
W	1·254	1·25	215
	1·245		522
	1·233		015
MS	1·232	1·23	$\bar{5}01$
	1·226		125
VVW	1·217	1·21	424
	1·201		315
W	1·199	1·20	440
	1·198		225
VW	1·182	1·186	523
	1·181		$\bar{1}05$
M	1·180	1·18	350
	1·179		025
VW	1·166	1·17	060
	1·166		044
M	1·164	1·163	$\bar{1}15$
	1·162		$\bar{5}21$
M	1·161	1·160	053
M	1·151	1·151	325
	1·151		$\bar{4}13$
W	1·148	1·148	160
	1·147		530
M	1·139	1·142	$\bar{3}14$
VW	1·123	1·131	602
M	1·114	1·114	611
VW	1·103	1·102	035
M	1·093	1·093	524
W	1·079	1·080	425
	1·070		613
M	1·069	1·068	622
	1·066		450
M	1·058	1·054	216
MS	1·038	1·039	505
M	1·027	1·028	515
M	1·0198	1·020	604
VW	1·008	1·007	614
VW	1·002	1·003	$\bar{5}13$
M	0·9977	0·996	$\bar{6}21$
	0·9952		525
M	0·9827	0·985	$\bar{3}15$
W	0·9784	0·978	624
W	0·9722	0·972	$\bar{5}23$
VW	0·9651	0·964	701
W	0·9592	0·961	550
M	0·9526	0·952	036
W	0·9330	0·933	055
W	0·9122	0·912	217
W	0·9002	0·896	$\bar{5}14$
W	0·8745	0·874	080
W	0·8654	0·867	606
W	0·8558	0·855	705
VW	0·8494	0·850	715
M	0·8451	0·845	734
W	0·8366	0·837	056
M	0·8239	0·824	800
W	0·8199	0·820	$\bar{5}53$
M	0·8137	0·814	$\bar{6}04$
W	0·8114	0·811	$\bar{5}15$
M	0·8061	0·806	$\bar{5}44$
MS	0·7993	0·799	660
M	0·7955	0·795	$\bar{5}25$
	0·7954		$\bar{4}16$
M	0·7934	0·793	$\bar{3}64$
MS	0·7917	0·791	474
MS	0·7829	0·783	008

SYMBOLS USED : M: Moderate (ly) ; S : Strong ; W : Weak ; V : Very.

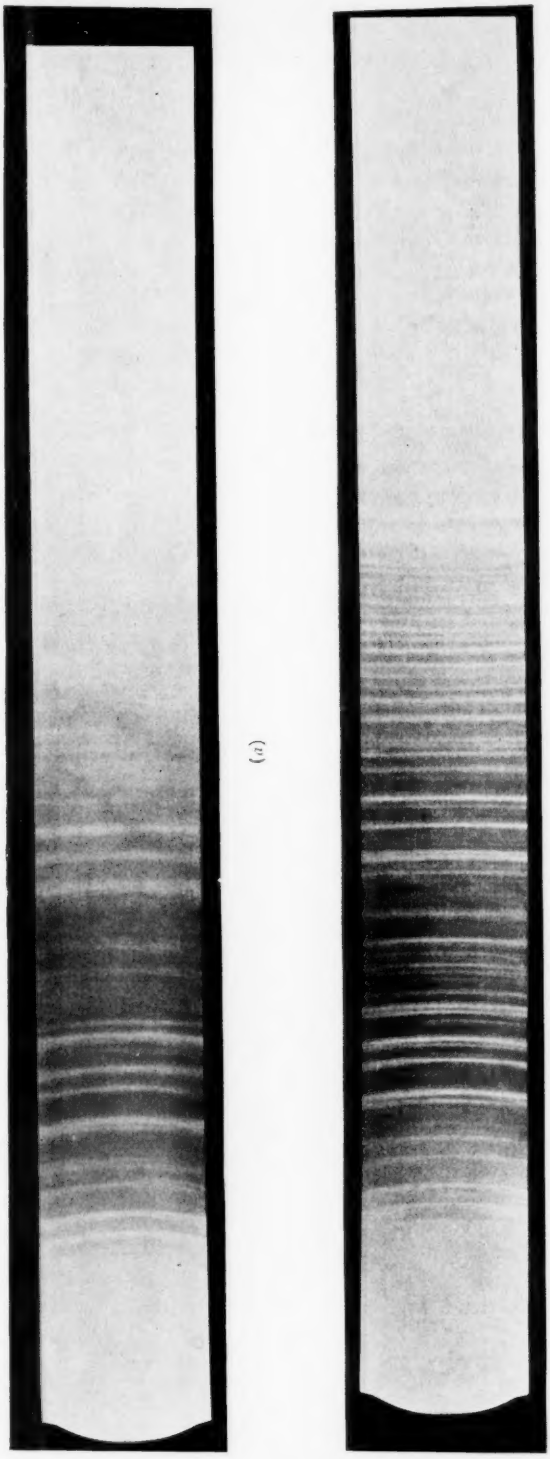

FIG. 1. X-ray Powder Diffraction Pattern: (*a*) Sample of natural monazite—untreated; (*b*) Same sample after heat treatment.

IV. Discussion

It can be seen from Fig. 1 (*a*) that the pattern obtained on the naturally occurring monazite is quite diffuse indicating the general absence of internal crystallinity which is regained on heat treatment as can be seen from the clear pattern of Fig. 1 (*b*). It is not possible at present to estimate the degree of metamictization of the mineral since the relationship between structure damage and the total alpha radiation is not known. This is further handicapped by the lack of definite knowledge of the position of the thorium ions in the structure and the effect of different amounts of thorium oxide and silica on the lattice dimensions. These points are being investigated.

In order to substantiate the findings of the X-ray investigation that the natural thorium-containing mineral is largely metamict a petrological examination was made. All the original samples were found to be weakly birefringent with most of the grains showing only the first order grey and only a few grains showing slightly higher colours. All the heated samples showed strong birefringence and the average refractive index was found to have increased to 1·83 from the original value of 1·79. Complete optical data were not obtained because of the fine grain size of the particles, and only an average index was measured. The average density of sample No. 1 increased from 5·33 to 5·62 g./cm.^{3} on heat treatment.

Summary

Monazite is commonly believed to be a nonmetamict mineral. The results of the published X-ray examination of monazite do not unambiguously support this belief. The results of the present investigation on four different samples of monazite of known thorium content show that the thorium-containing monazite occur in a fairly high degree of metamictization. The results of the petrological examination also support this conclusion.

Acknowledgement

The authors thank the Director, National Chemical Laboratory, for permission to carry out the X-ray work in that laboratory.

Bibliography

1. v. Gliszczynski, S. .. *Zeit. Krist.*, 1939, **101**, 1.
2. Hurley, P. M. and Fairbairn, H. W. *Geol. Soc. Amer. Bull.*, 1953, **64**, 659.
3. Hutton, C. O. .. *Ibid.*, 1950, **61**, 635.
4. Pabst, A. .. *Amer. Mineral*, 1951, **36**, 60.
5. Parrish, W. .. *Ibid.*, 1939, **24**, 651.
6. Ramdohr, P. .. *Klochmann's Lehrbuch der Mineralogie*, Stuttgart, 1936.

PROMINENCE ACTIVITY (1905-1952)

By R. Ananthakrishnan, F.A.Sc.

(From the Regional Meteorological Centre, Sonegaon Aerodrome, Nagpur)

Received June 28, 1954

1. Introduction

In the field of prominence statistics the Kodaikanal Observatory has a large collection of uniformly worked out data commencing from 1905 till the present time. Since the Memoir published by Mr. and Mrs. Evershed (1917) in which they considered the Kodaikanal prominence data upto 1914, additional data for four more decades have been accumulated. About the time that the Jubilee commemorating fifty years of work of the observatory was celebrated in 1951, the present writer who was working as Assistant Director of the observatory till very recently felt that the time was opportune to undertake a general review and discussion of the prominence data collected since the inception of the observatory, and a detailed survey of the results of solar prominence observations made at Kodaikanal was, therefore, commenced. The material for the study was largely original data contained in a number of registers. (The half-yearly summaries of prominence observations published in the Bulletins of the Kodaikanal Observatory are based on the detailed tabulations maintained in these registers.) The scope of the study embraced both limb and disc prominences (dark markings). As the work progressed, it was felt convenient to deal with it in parts. The first part entitled *Discussion of the Results of Observations of Solar Prominences made at Kodaikanal from* 1904 *to* 1950 is under publication as Bulletin No. 137 of the Kodaikanal Observatory.* This paper which deals only with limb prominences gives an account of the methods of observation and evaluation and also incorporates detailed tables of the distribution of mean daily profile areas of prominences according to heliographic latitudes year by year for the period 1905 to 1950. Various aspects of prominence activity during the period such as comparison of the northern and southern hemispheres, life-history of the low and high latitude prominences, the east-west distribution of prominences, the distribution of " metallic " prominences, etc., are considered in the paper.

* This will be referred to as Paper I in what follows.

In connection with the work referred to in the preceding paragraph, a set of charts of prominence activity were also prepared.† Unfortunately, these diagrams could not be incorporated in Paper I. In the meanwhile, data for two more years became available so that the charts could be extended incorporating the data upto the end of 1952. It is felt that these diagrams which summarise quantitatively a vast mass of prominence data and bring out strikingly the salient features of prominence activity during the last four solar cycles might be of interest to workers in the field of solar physics and perhaps also of geophysics. They represent in three different ways the trend of prominence activity in relation to the sunspot cycle for the period 1905 to 1952. The object of this paper is to present these charts and to give a brief discussion of some of the features brought out by them.

2. Distribution of Profile Areas of Prominences according to Heliographic Latitudes

At Kodaikanal, prominence activity has been reckoned from the very beginning both in terms of the *numbers* of individual prominences observed at the limb as well as in terms of the *profile areas* of the prominences. For details of the methods of evaluation reference may be made to Paper I. For reasons discussed in that paper the Kodaikanal prominence numbers do not constitute a good index of prominence activity. The mean daily profile area of prominences, on the other hand, is a recognised representative index of prominence activity. The values of this quantity for five-degree intervals of latitude for the NE, NW, SE and SW limbs during the years 1905 to 1950 are listed in Table I of Paper I. Similar data for the years 1951 and 1952 are given in Table I of the present paper. The unit of prominence area for this table is 10^{-3} square minute of arc. (The figures in the table have to be divided by 4·65 in order to express the areas in terms of the international unit of prominence area which is the area of a rectangle whose height is 1 second of arc of the celestial sphere and whose base is 1 degree along the solar limb.)

To give an idea of the representative nature of the prominence statistics of Kodaikanal for the period 1905 to 1952, the number of " effective " days of observation for the individual months as well as for the individual years is listed in Table II. The *effective* days are in general somewhat less than the *total* number of days of observations since spectroheliograms for days when the sky and seeing conditions are not good, are given a weightage

† Some of these diagrams were shown at the Annual Meeting of the Indian Academy of Sciences held at Trivandrum in December, 1952.

TABLE 1

Distribution of Mean Daily Prominence Areas according to Heliographic Latitudes

NORTH

Year / No. of days	Total	85—90	80—85	75—80	70—75	65—70	60—65	55—60	50—55	45—50	40—45	35—40	30—35	25—30	20—25	15—20	10—15	5—10	0—5
1951 NE	769	0	0	0	1	1	2	5	14	40	84	103	117	120	68	63	57	48	46
338 NW	724	0	0	0	1	1	1	5	13	29	64	80	105	114	74	73	56	68	40
N	**1493**	**0**	**0**	**0**	**2**	**2**	**3**	**10**	**27**	**69**	**148**	**183**	**222**	**234**	**142**	**136**	**113**	**116**	**86**
1952 NE	423	0	1	0	1	0	1	3	13	27	33	39	41	49	50	46	46	44	29
342 NW	557	0	0	0	1	1	1	1	6	26	57	74	83	70	62	43	42	46	44
N	**980**	**0**	**1**	**0**	**2**	**1**	**2**	**4**	**19**	**53**	**90**	**113**	**124**	**119**	**112**	**89**	**88**	**90**	**73**

SOUTH

0—5	5—10	10—15	15—20	20—25	25—30	30—35	35—40	40—45	45—50	50—55	55—60	60—65	65—70	70—75	75—80	80—85	85—90	Total	Year / No. of days
36	46	65	79	117	101	60	53	49	21	6	1	0	0	0	0	0	0	634	SE 1951
45	61	53	57	74	76	80	69	55	31	11	4	2	0	1	0	0	0	619	SW *338*
81	**107**	**118**	**136**	**191**	**177**	**140**	**122**	**104**	**52**	**17**	**5**	**2**	**0**	**1**	**0**	**0**	**0**	**1253**	**S**
35	38	46	33	31	42	70	102	55	15	1	1	1	1	0	0	0	0	471	SE 1952
43	54	62	47	52	62	74	81	36	8	4	1	0	0	0	0	0	1	525	SW *342*
78	**92**	**108**	**80**	**83**	**104**	**144**	**183**	**91**	**23**	**5**	**2**	**1**	**1**	**0**	**0**	**0**	**1**	**996**	**S**

TABLE II

Effective Number of Days of Prominence Observations

Year \ Month	J.	F.	M.	A.	M.	J.	J.	A.	S.	O.	N.	D.	I	II	Total
1905 ..													150	134	284
06 ..													150	103	253
07 ..													165	131	296
08 ..													158	140	298
09 ..													159	137	296
10 ..													164	141	305
1911 ..													157	129	286
12 ..							14	19	23	18	16	24	159	114	273
13 ..	23	25	30	28	26	21	18	23	26	22	18	22	153	129	282
14 ..	28	27	29	29	26	19	11	20	22	16	24	20	158	113	271
15 ..	27	27	30	30	30	19	15	21	20	26	19	21	163	122	285
16 ..	31	27	30	27	28	16	28	27	22	23	26	26	159	152	311
17 ..	22	25	28	27	29	17	20	22	20	21	19	27	148	129	277
18 ..	25	26	30	27	19	24	23	19	24	25	12	19	151	122	273
19 ..	29	28	30	26	25	21	15	22	15	22	17	24	159	115	274
20 ..	25	29	30	27	28	20	18	23	25	21	13	29	159	129	288
1921 ..	22	26	31	29	30	23	16	24	22	21	24	25	161	132	293
22 ..	28	22	31	27	23	22	15	22	22	19	16	29	153	123	276
23 ..	26	28	27	28	29	23	15	19	21	17	25	17	161	114	275
24 ..	27	27	29	28	27	24	27	27	27	27	27	26	162	161	323
25 ..	29	28	29	27	27	23	24	23	28	27	23	27	163	152	315
26 ..	31	28	31	30	29	27	29	27	27	29	25	30	176	167	343
27 ..	29	27	28	29	28	24	24	23	26	27	26	30	165	156	321
28 ..	24	28	29	26	30	26	26	25	28	26	18	26	163	149	312
29 ..	30	25	31	27	27	21	25	29	29	28	26	28	161	165	326
30 ..	29	28	27	29	29	26	24	26	27	26	26	28	168	157	325

TABLE II—(*Contd.*)

Year \ Month	J.	F.	M.	A.	M.	J.	J.	A.	S.	O.	N.	D.	I	II	Total
1931 .	28	28	31	28	28	29	28	29	29	29	25	20	172	160	332
32 ..	30	27	30	29	29	29	29	28	29	28	26	25	174	165	339
33 ..	28	27	30	27	27	27	28	28	27	24	25	29	166	161	327
34 ..	27	28	30	28	29	25	25	25	28	23	24	24	167	149	316
35 ..	26	27	29	26	29	27	24	24	27	25	23	24	164	147	311
36 ..	29	28	28	29	27	24	23	23	27	28	25	26	165	152	317
37 ..	26	27	30	28	30	26	25	28	28	28	24	29	167	162	329
38 ..	30	25	29	28	30	26	23	25	24	25	26	23	168	146	314
39 ..	27	27	31	24	28	22	16	22	26	23	26	28	159	141	300
40 ..	29	28	29	29	31	30	28	29	26	26	21	28	176	158	334
1941 ..	26	25	26	27	25	23	28	27	27	24	21	26	154	153	307
42 ..	29	27	28	28	28	22	27	29	28	28	28	27	162	167	329
43 ..	27	24	29	26	25	24	23	25	25	25	23	21	155	142	297
44 ..	26	22	19	26	28	26	26	29	28	28	19	22	147	152	299
45 ..	23	19	25	22	24	24	27	27	26	26	26	24	137	156	293
46 ..	30	26	30	29	26	25	25	28	25	24	19	20	166	141	307
47 ..	26	24	29	26	28	26	26	25	27	27	27	25	159	157	316
48 ..	29	24	30	27	28	30	25	28	28	27	25	25	168	158	326
49 ..	27	26	29	27	25	28	28	31	29	29	29	29	162	175	337
50 ..	27	27	29	28	29	29	28	28	26	27	28	30	169	167	336
1951 ..	29	27	30	28	31	27	27	31	29	29	22	28	172	166	338
52 ..	27	27	29	29	28	29	27	27	31	30	31	27	169	173	342
Total ..													7743	6974	14717

(For the period prior to July 1912, the number of effective days for the individual months is not available in the Kodaikanal records.)

of $\frac{3}{4}$ or $\frac{1}{2}$ only depending upon the quality. In general, the observing conditions for solar work are better at Kodaikanal during the first half of the

year than during the second half when the station comes under the influence of the south-west and north-east monsoons.

Upto 1923 the prominence data of Kodaikanal are based on the observations made at this observatory only. Thereafter the Kodaikanal data have been supplemented with data derived from photographs obtained from the Mt. Wilson and Meudon Observatories for the days on which Kodaikanal photographs were either of inferior quality or not available, on account of unfavourable weather conditions. This accounts for the generally greater number of effective days of observation per year since 1923. Comparison of the figures in the columns headed I and II in Table II for the years before and after 1923 shows that the number of foreign photographs required to supplement the Kodaikanal data is more during the second half of the year than during the first half.

The charts in Fig. 1 give a pictorial representation of the distribution of mean daily prominence areas round the limb of the sun year by year from 1905 to 1952. For the years 1907 to 1911 the data for the east and west limbs are not separately available in the Kodaikanal records for the north and south hemispheres. Hence, for these years the total areas for the five-degree zones have been divided by 2 and depicted symmetrically on the east and west limbs so that the diagrams for these years may have a uniform appearance with those for the remaining years. The original diagrams were drawn on a scale of 1 inch to the solar radius; also 1 inch was taken to represent 1/10 square minute of prominence area. The prominence area for each five-degree zone is represented by a radial line of appropriate length originating from the centre of the zone. As all the diagrams are drawn to the same scale and as a uniform practice has been followed at Kodaikanal for evaluation of prominence areas, the diagrams for the different years are mutually comparable quantitatively.

3. Isopleths of Mean Daily Prominence Areas

To bring out strikingly the manner in which prominence activity varies in the course of the sunspot cycle, the mean daily profile areas for five-degree latitude zones in the two hemispheres were entered on graph paper with the years as abscissae and heliographic latitudes as ordinates. The profile area corresponding to a particular five-degree interval of latitude was entered against the mean latitude of the zone. Contour lines were then drawn at intervals of 50×10^{-3} square minute of prominence area using linear interpolation between adjacent plotted values. The resulting diagram is reproduced as Fig. 2 in which the intervals corresponding to the different degrees of prominence activity are clearly demarcated. The curve of Zürich

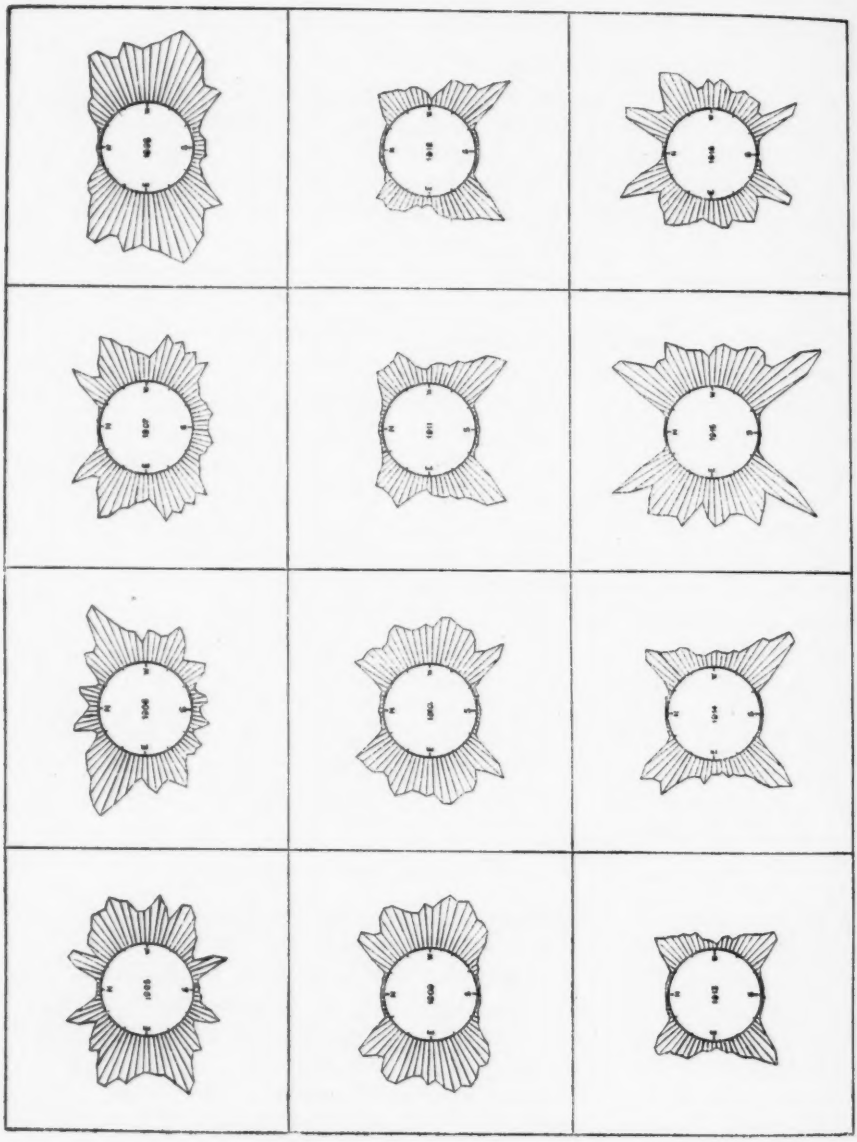

FIG. 1 (*a*).
DISTRIBUTION OF PROMINENCE AREAS ACCORDING TO HELIOGRAPHIC LATITUDES (1905–1916)

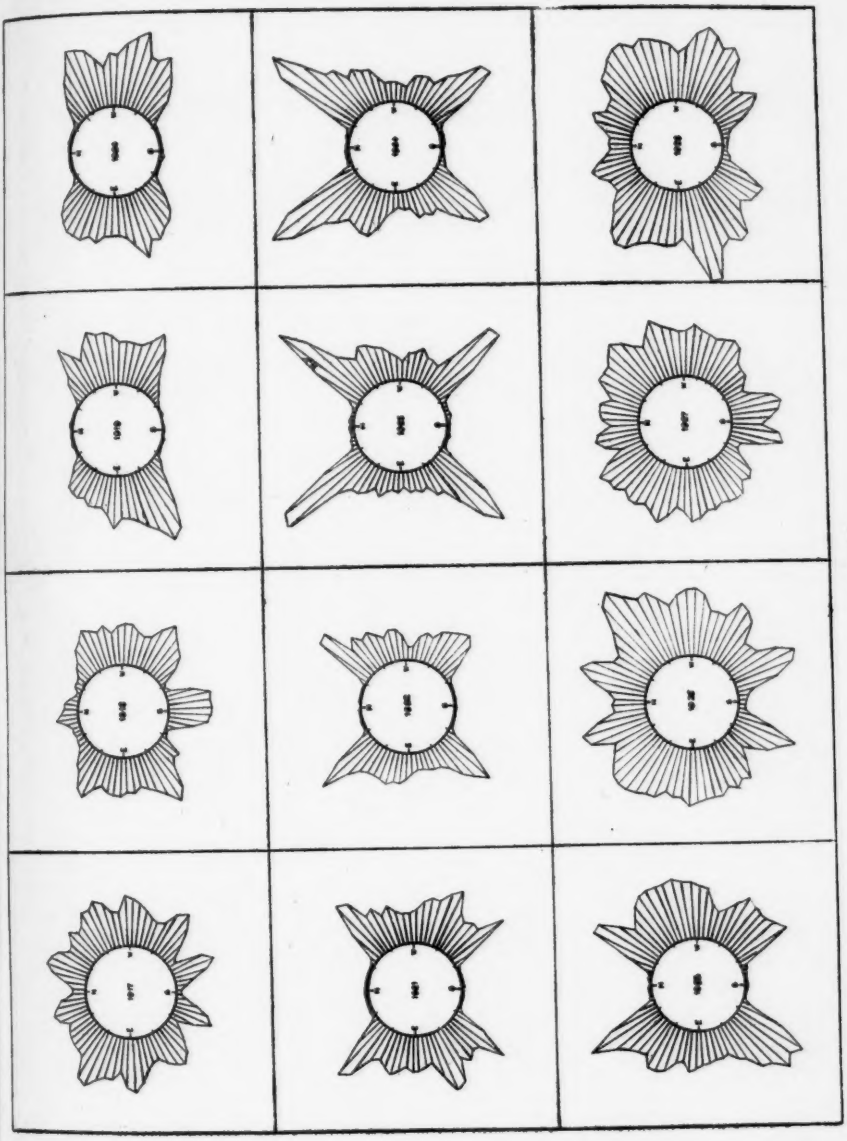

FIG. 1 (*b*)
DISTRIBUTION OF PROMINENCE AREAS ACCORDING TO HELIOGRAPHIC LATITUDES
(1917–1928)

DISTRIBUTION OF PROMINENCE AREAS ACCORDING TO HELIOGRAPHIC LATITUDES
(1905–1916)

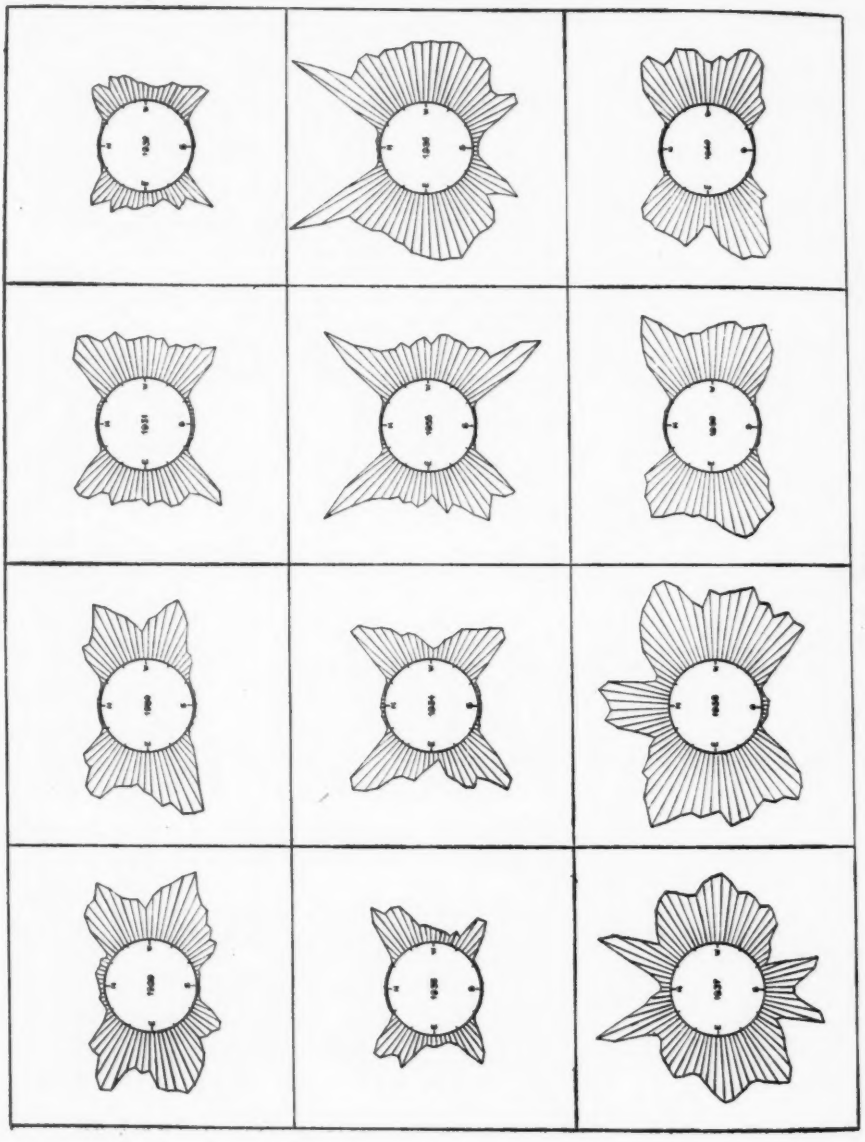

FIG. 1 (c)
DISTRIBUTION OF PROMINENCE AREAS ACCORDING TO HELIOGRAPHIC LATITUDES (1929–1940)

DISTRIBUTION OF PROMINENCE AREAS ACCORDING TO HELIOGRAPHIC LATITUDES
(1929–1940)

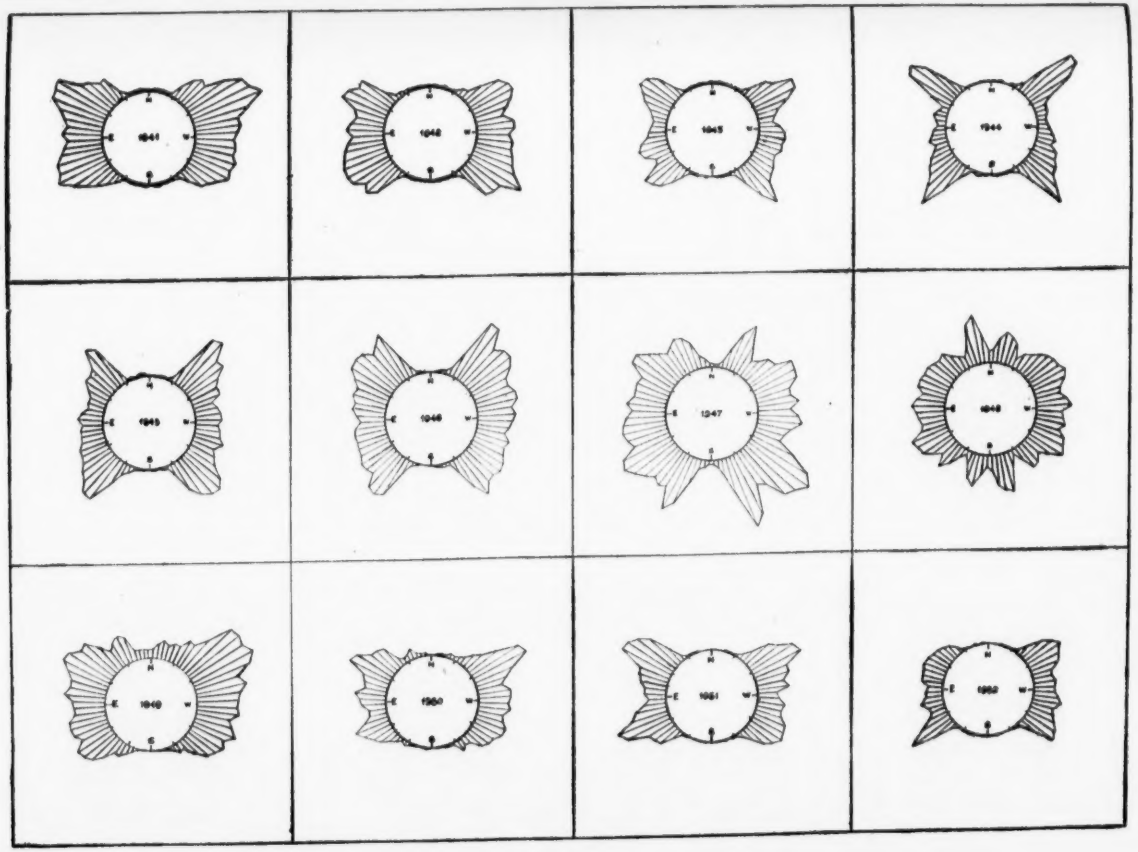

FIG. 1 (*d*)
DISTRIBUTION OF PROMINENCE AREAS ACCORDING TO HELIOGRAPHIC LATITUDES
(1941–1952)

relative sunspot numbers for the period covered by the prominence observations is given at the top of the diagram. A similar diagram was contained in a note entitled " Prominence Activity and the Sunspot Cycle " published some time back (Ananthakrishnan, 1952).

4. Zonal Variation of Prominence Activity

Figures 3 (*a*) and 3 (*b*) illustrate the variation of prominence activity in each five-degree zone for the northern and southern hemispheres during the period 1905 to 1952. The zero of the vertical scale has been appropriately displaced to avoid superposition of the curves for the different latitude zones. The horizontal line against which the designation of a particular zone is written corresponds to the zero of prominence activity for that zone. The scale of prominence areas is indicated for the zone 0–5° at the bottom of the diagram and is the same for all the other zones. As in the case of the isopleth diagram, the curve of Zürich relative sunspot numbers is given at the top of each of the diagrams. The broken curve which runs close to the sunspot curve in the two diagrams represents the mean daily sunspot areas for the two hemispheres, the values of which were obtained from the Greenwich Photoheliograph Results.

5. Prominence Activity and the Sunspot Cycle

It is well known that sunspot activity is confined to two fairly well defined zones extending from the solar equator to about 40° latitude in either hemisphere. The commencement of a new solar cycle is heralded by the appearance of spots near about latitude $\pm$ 40°. As the cycle advances the centre of spot activity shifts progressively towards lower latitudes until towards the close of the cycle the spot activity wanes off near the solar equator while spots of the new cycle begin to appear at higher latitudes.

As contrasted with sunspots, prominences occur at all latitudes on the sun. However, in respect of the manner in which prominence activity manifests itself, we can divide each solar hemisphere into two zones, *viz.*, (*i*) a low latitude zone extending from the equator to about 40° and therefore practically coinciding with the sunspot zone, and (*ii*) a high latitude zone extending from 40° to the poles.

Prominences always occur in the low latitude zones although the activity is a minimum at the minimum epoch of the sunspot cycle. Prominence activity in the high latitude zones above latitude 60° is conspicuous only at and near the time of sunspot maximum. The activity dies down very rapidly thereafter. These broad features of prominence activity first established through the pioneering researches of Secchi and Respighi and sub-

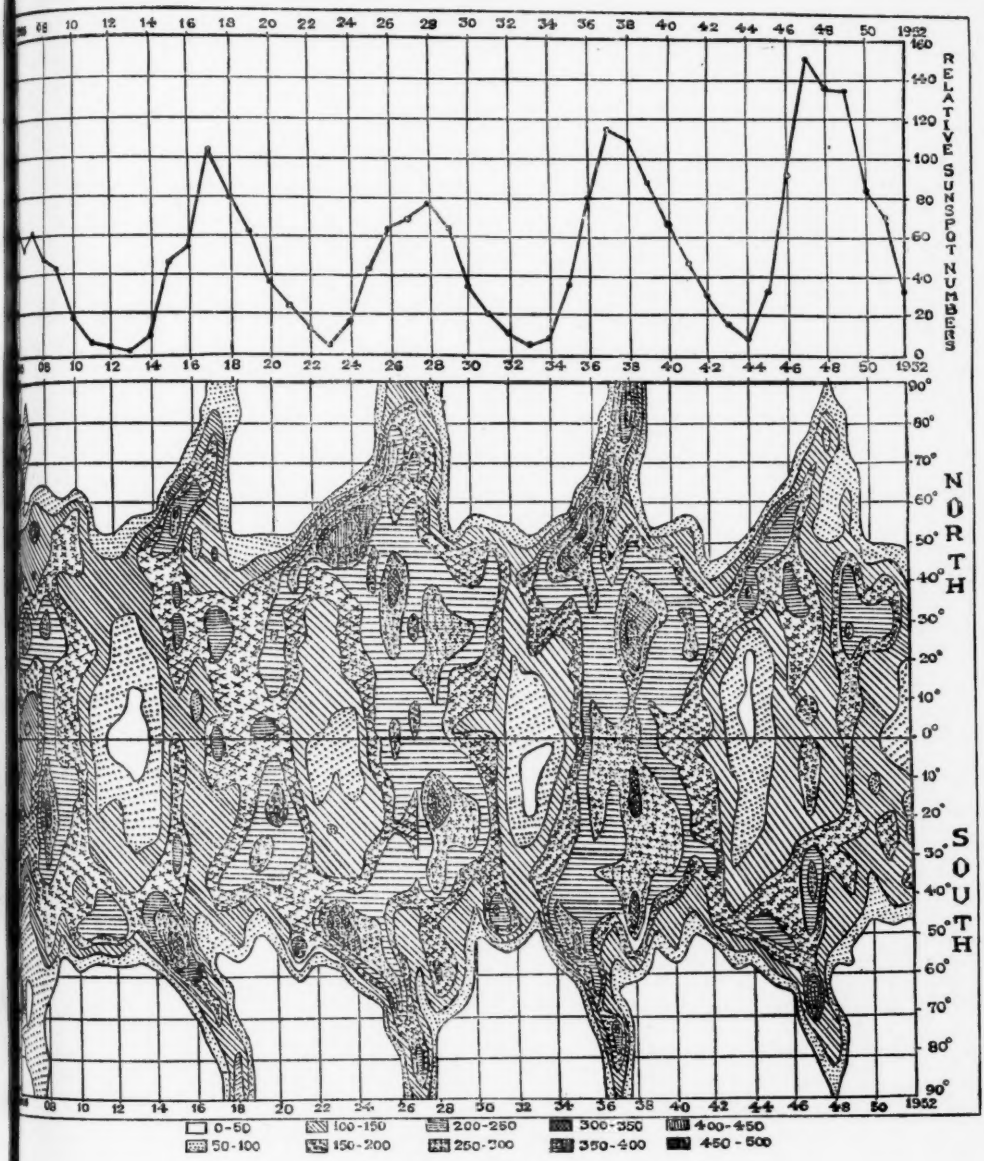

FIG. 2

Isopleths of mean Daily Prominence Areas (Unit: 10^{-3} sq. min.)
PROMINENCE ACTIVITY AND THE SUNSPOT CYCLE

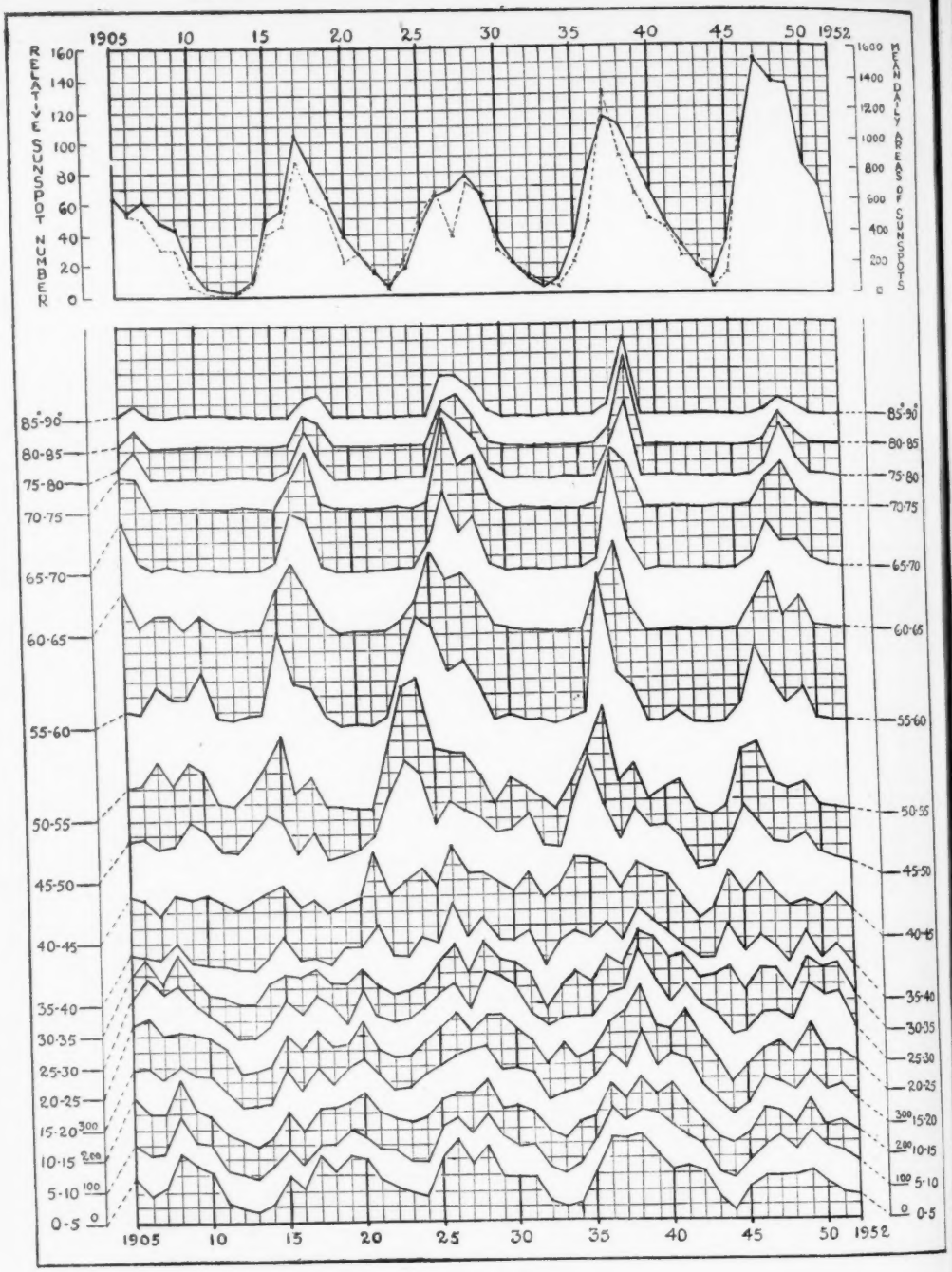

FIG. 3 (*a*)
VARIATION OF PROMINENCE ACTIVITY IN FIVE-DEGREE LATITUDE ZONES
(Northern Hemisphere)

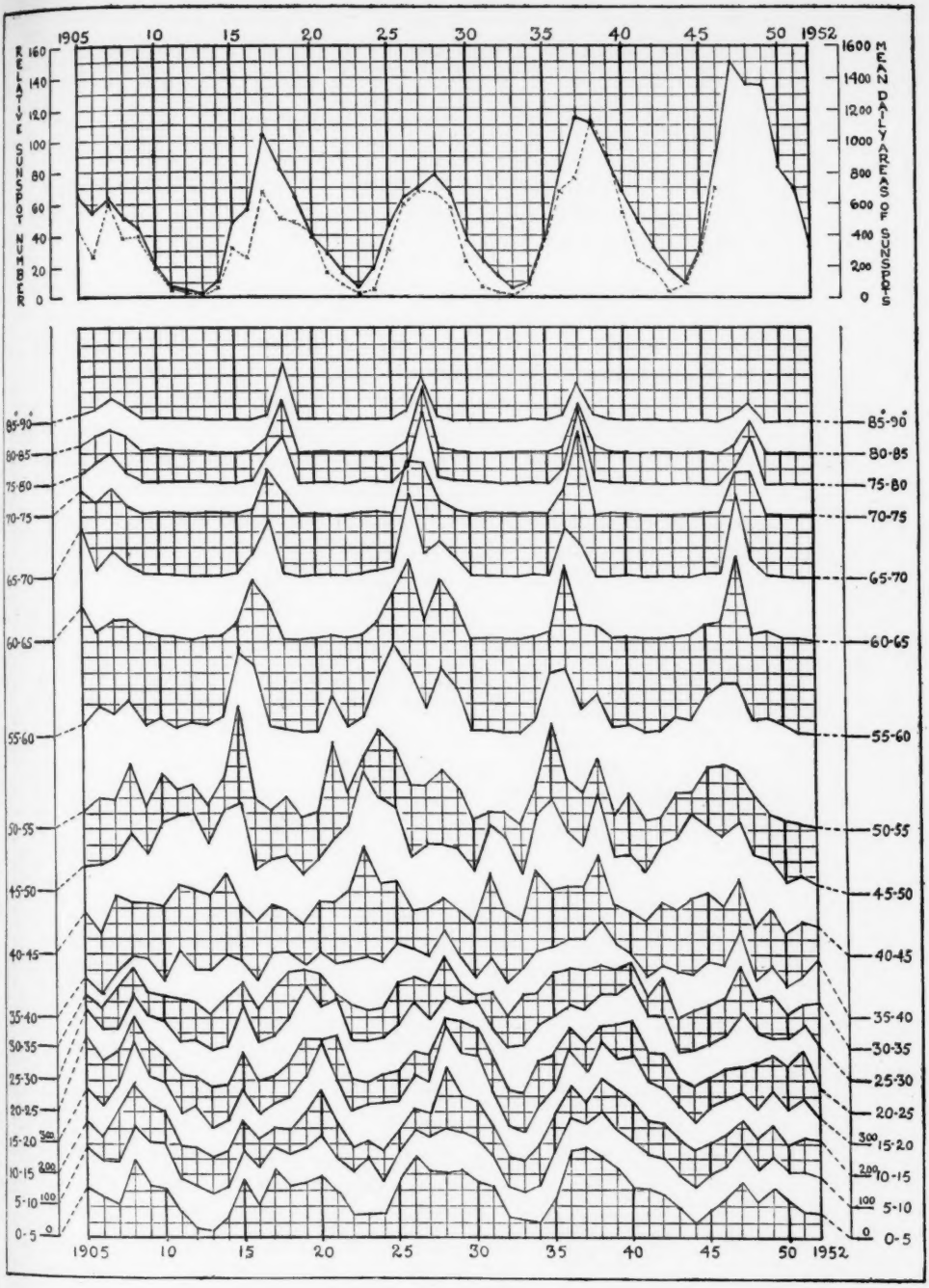

FIG. 3 (*b*)

VARIATION OF PROMINENCE ACTIVITY IN FIVE-DEGREE LATITUDE ZONES
(Southern Hemisphere)

sequently corroborated by the investigations of Ricco (1891, 1914), Lockyer (1903), Evershed (1917), Bocchino (1933), Baroccas (1939), Moss (1946) and D'Azambuja (1948), are clearly brought out by the diagrams which illustrate the present paper for each of the four cycles of solar activity covered by the period under study.

The manner in which prominence activity develops and progresses in the low and high latitude zones has been discussed by several workers. Although there is general agreement as regards the high latitude zones there is not such a consensus of opinion about the trend of activity in the low latitude or sunspot zones. According to Evershed, prominence activity begins to develop in the high latitude zones between 40° and 50° soon after sunspot minimum. With increasing sunspot activity the centres of high latitude prominence activity gradually move polewards until near the epoch of sunspot maximum there is a rapid rush towards the poles. The high latitude prominence activity suddenly disappears soon after sunspot maximum. These features are clearly illustrated by the figures which accompany the present paper.

The trend of activity in the low latitude zone is not so clearly defined because of irregularities caused by the co-existence of several active centres. From his observations Evershed concluded that in the sunspot zones prominence activity drifts more or less in phase with the sunspots from higher latitudes towards the equator and dies out near the lowest latitude reached by sunspots at the time of sunspot minimum. Lockyer and Lockyer (1903) concluded from their study of the Italian prominence data for the period 1872 to 1901 that the low latitude prominence activity is centred round latitude $\pm 24°$ where the activity begins to manifest itself shortly after sunspot minimum. With the ascending phase of the sunspot cycle there is a corresponding rise in prominence activity in the sunspot zone without appreciable shift of the centre of activity. Finally the centres of prominence activity recede and merge with the high latitude zones at about $\pm 40°$ before sunspot minimum. Thus it will be seen that the conclusions of Evershed and those of Locyker and Lockyer are rather divergent in respect of the growth and progress of prominence activity in the sunspot zones.

To get a better insight into the nature of latitudinal migration of prominences M and M^{me} D'Azambuja made a large number of measurements on long-lived H-alpha dark markings (prominences seen in projection on the disc) over the elven-year period 1919 to 1930 which covered both the ascending and descending phases of the sunspot cycle. Their measurements led them to conclude that *on the average* all prominences have a slow pole

ward drift in both the hemispheres. The rate of pole-ward drift was found to be about 2° per solar rotation near the equator and decreased progressively to about 1° per solar rotation near latitude 50°. It was also found that the rate of pole-ward drift was at least twice as rapid in the ascending phase of the sunspot cycle than in the descending phase particularly in the high latitude zones. Based on these findings, M and Mme D'Azambuja have advanced the view that all prominences originate in the sunspot zones and migrate towards higher latitudes, thus indicating the existence of a meridional circulation on the sun which is postulated by certain solar theories.

While the meridional movement of high latitude prominences at the rate of about 1° per solar rotation is clearly brought out by the diagrams reproduced here, the statistical study of prominences fails to give direct evidence about the pole-ward migration of prominences in the low latitude zones. From an examination of Figs. 3 (*a*) and 3 (*b*) it will, however, be seen that the amplitude of variation of prominence activity in the five-degree intervals of the sunspot zones decreases with increasing latitude and is least at the outer boundaries of the zones. It will also be seen that in the high latitude zones the progress of prominence activity from 70° to the poles is more rapid than the progress from 45° to 70°. For a fuller discussion of the significance of these features reference may be made to Paper I.

6. Prominence Activity and the Solar Corona

In a series of papers Dr. Lockyer (1903, 1922, 1931) has shown that there is an intimate connection between the distribution of prominences round the solar limb and the forms of the corona. He has classified the different forms of the corona into three main types, *viz.*, (i) " polar " or maximum type; (ii) " equatorial " or minimum type; and (iii) the " intermediate " type. In the ploar type, the coronal streamers are found all round the solar disc and the polar rifts are absent. It is usually known as the maximum sunspot type. In the equatorial type of corona the streamers are restricted to low solar latitudes and the polar rifts are conspicuous. This type which occurs at the time of minimum sunspot activity is also called the " wind-vane " or " fish-tail " form of corona. As its name suggests, the intermediate corona forms a transition between the polar and the equatorial types. In it the streamers occur at mid-solar latitudes and the rifts though present are less extensive and the equatorial extensions less pronounced as compared with the minimum type.

From his study of the coronal drawings and photographs obtained during the total solar eclipses for the period 1870 to 1930, Dr. Lockyer found

that the polar type corona occurs only when prominence activity is pronounced at high latitudes in one or both the hemisphers of the sun. As we have already seen this occurs only at or near the epoch of sunspot maximum. The equatorial forms of the corona occur when the prominence activity is confined to the lowest latitudes which occurs near the epoch of minimum sunspot activity. Lockyer distinguishes between two types of intermediate coronal forms, " intermediate up " and " intermediate down " corresponding to the waxing and waning phases of the sunspot cycle.

An examination of the charts showing the distribution of prominences according to heliographic latitudes reproduced in Fig. 1 bears out the rather striking similarity between the prominence distribution round the solar limb and the coronal forms considered above. A question which naturally arises is, whether the coronal forms are to be correlated more directly with sunspot activity or with prominence activity. There is some difference of opinion on this point. Ludendorff (1928) and Mitchell (1929) have suggested that the coronal form is governed by sunspot action while Lockyer (1931) and Bergstrand (1930) incline to the view that there is more direct connection between prominence distribution on the sun and the forms of the corona. In this connection an observation of Evershed which has been quoted by Lockyer is of interest. In the Memoir on " Results of Prominence Observations ", Evershed examined the connection between the distribution of prominences with the types of corona and found that Lockyer's theory generally agreed with observations except in the case of the corona of 1908 January 3. As we see from Fig. 1, prominence activity in the southern hemisphere enveloped the pole during 1907 and 1908, but in the northern hemisphere the activity practically stopped beyond 65°. According to Lockyer's theory the coronal streamers should be more pronounced over the south polar region than over the north. However, from the illustration of the corona given in McClean's Report it appeared that streamers were developed almost all round the disc except at the south pole. Evershed remarked that " if Mr. McClean's corona is correctly oriented, therefore, the distribution of streamers in the polar regions does not agree with the distribution of prominences at that time". At a later date Evershed discovered that the north and south poles had been interchanged in the picture of the corona; the apparent contradiction with Lockyer's theory, therefore, disappeared.

Although various forms of solar activity closely follow the sunspot cycle the exact nature of the causal relationships between them are at present only very imperfectly known. Nevertheless, it would appear that the coronal forms are more directly related to the distribution of prominences than of sunspots.

7. Solar Activity during the Latest Cycle

Judged by sunspot activity the latest solar cycle which attained a maximum in 1947 is one of the most active. This cycle has also the unique distinction of having been characterised by some of the biggest spot groups on record. But examination of Figs. 1, 2 and 3 reveals that prominence activity has been less pronounced during this cycle as compared with the two previous ones in which spot activity reached the peak in 1937 and 1928. In this connection it is significant that Behr and Siedentoff (1952) and Kleczek (1953) found that solar flare activity has also been less during the latest cycle as compared with the previous one. The trend of geomagnetic activity during the maximum epochs of the last four solar cycles indicates that the latest cycle has been geomagnetically the least active (Ananthakrishnan, 1953). In fact a preliminary examination suggests that during the maximum phase of the sunspot cycle geomagnetic activity shows a better correlation with prominences than with sunspots.

8. Acknowledgements

The author's thanks are due to all members of the Kodaikanal Observatory staff, past and present, who have participated in the collection of the large mass of prominence data. Mr. P. Madhavan Nayar, Professional Assistant of the Kodaikanal Observatory who collaborated in the present work and is co-author of Paper I, assisted in preparing the charts reproduced in Fig. 1. The help of Mr. D. K. Das of the Meteorological Office, Nagpur, in tracing and inking Fig. 2 from the original prepared by the author is also acknowledged with thanks.

Summary

The paper illustrates with a series of diagrams the variation of prominence activity during the period 1905 to 1952 based on the prominence statistics collected at the Kodaikanal Observatory. The main features of prominence activity brought out by these diagrams are briefly discussed.

References

1. Ananthakrishnan, R. .. *Nature*, 1952, **170**, 156.
2. ———— .. *Ibid.*, 1953, **172**, 854.
3. Barocas, V. .. *Ap. J.*, 1939, **89**, 486.
4. Behr, A. and Siedentopf, H. .. *Z. f. Ap.*, 1952, **30**, 177.
5. Bergstrand, O. .. *Ark. f. Mat. Astr. O. Fys.* A, 1930, **22** No. 1.
6. Bocchino, G. .. *M.S.A. Ital.*, 1933, **6**, 479.
7. D'Azambuja, L., M and Mme. .. *Ann. d. Obs. Paris*, 1948, **6**, Fas. 7.
8. Evershed, J. and Evershed, M. A. *Mem. Kod. Obs.*, 1917, **1**, Part 2.

9. Kleczek, J. .. *Bull. Ast. Inst. Czechoslovakia*, 1953, **4**, 9.
10. Lockyer, N. and Lockyer, W. J. S. *M.N.R.A.S.*, 1903, **63**, 446.
11. Lockyer, W. J. S. .. *Ibid.*, 1903, **63**, 481.
12. ———— .. *Ibid.*, 1922, **82**, 323.
13. ———— .. *Ibid.*, 1931, **91**, 797.
14. Ludendorff, H. .. *Sitz. d. Preuss. d. Wiss. Phys. Math. Klasse*, 1928, **16**.
15. Mitchell, S. A. .. *Hand. d. Ap.*, 1929, **4**, 338.
16. Moss, W. .. *Ann. Sol. Phys. Obs. Cambridge*, 1946, **3**, Part 3.
17. Ricco, A. .. *M.S. Sp. Ital.*, 1891, **20**, 135.
18. ———— .. *Ibid.*, (2nd Series), 1914, **3**, 17.

KINETICS OF THE OLEFINE-BROMINE REACTION

*Part VIII. The Catalysed Reaction between Bromine and Crotonic and Dimethylacrylic Acids in Carbon Tetrachloride Solutions

By I. M. Mathai and S. V. Anantakrishnan, F.A.Sc.

(Department of Chemistry, Madras Christian College, Tambaram)

Received May 29, 1954

In earlier parts of this series[1] the reaction had been studied in glacial acetic acid solution and a good homogeneous reaction had generally been obtained using hydrogen bromide as the catalyst. Venkatraman[2] had reported that iodine halides catalyse the reaction. The previous part contained a report of our observations in carbon tetrachloride which showed a pronounced heterogeneous reaction and it was considered worth while studying the influence of iodine halides and pyridine.

Experimental

The experimental technique adopted was the same as in the previous parts, solvents and reagents being purified by the same process. Iodine chloride and iodine bromide were B.D.H. products fractionated after drying while A.R. Pyridine was dried over sticks of KOH and distilled before use (b.p. 115° C./760 mm.).

Typical runs are presented in Tables I and II and Figs. 1 and 2.

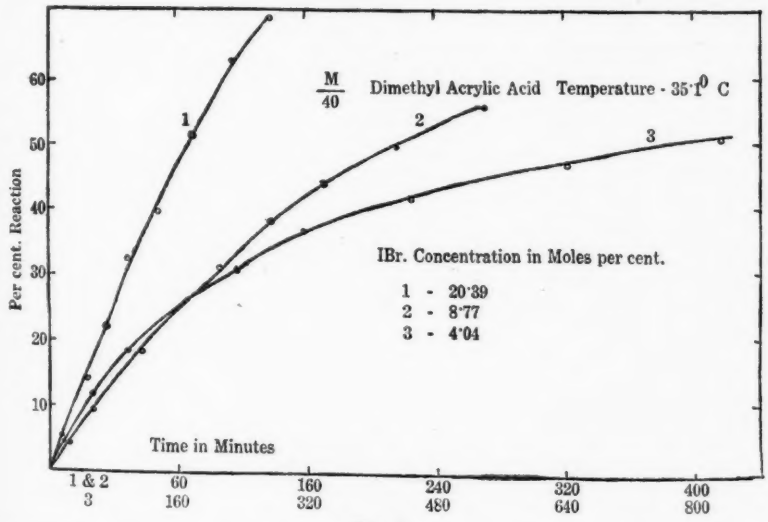

Fig. 1

* Based on thesis of I.M.M. approved for the M.Sc. degree of Madras University.

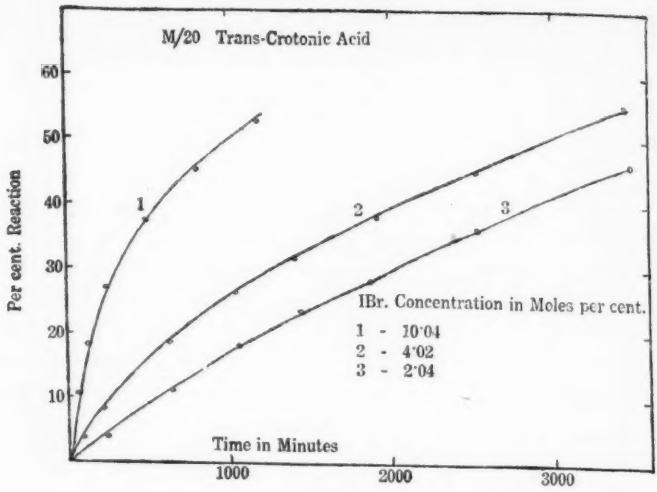

FIG. 2

TABLE I. *Catalysed Reaction between Bromine and Dimethyl Acrylic Acid*

Concentration of Reactants and temp.	Catalyst	Catalyst Bromine moles %							
M/15 at 30° C.	IBr	5·712	Time	0	4·38	8·28	10·78	14·00	21·22	37·6
			Titre	11·15	9·80	8·60	8·00	7·00	5·90	4·55
			% Reaction	0	12·85	24·29	30·00	39·72	50·00	62·85
		3·087	Time	0	1·97	3·82	7·45	11·42	18·07	28·20
			Titre	10·5	9·50	9·00	7·90	7·00	5·80	5·10
			% Reaction	0	6·12	11·23	21·43	31·63	43·88	51·02
		1·528	Time	0	2·58	4·45	9·98	13·92	22·00	37·98
			Titre	10·5	9·70	9·10	7·70	6·80	6·05	4·70
			% Reaction	0	3·54	9·60	23·74	32·83	40·41	54·63
	ICl	3·068	Time	0	1·97	72·25	79·50	88·67	95·97	126·9
			Titre	10·00	9·90	9·10	8·15	6·85	6·10	4·72
			% Reaction	0	1·03	9·27	20·10	32·44	40·21	53·60
		1·511	Time	0	22·55	47·10	59·35	74·58	104·5	
			Titre	10·00	9·70	8·90	7·40	6·15	4·80	
			% Reaction	0	3·06	11·17	26·40	39·09	52·79	
M/20 at 35° C.	IBr	3·992	Time	0	2·07	5·33	9·52	11·50	16·25	25·92
			Titre	9·60	9·20	8·50	7·40	6·60	5·80	4·50
			% Reaction	0	4·26	11·70	23·42	31·92	40·42	54·26
		0·9982	Time	0	2·20	4·87	8·88	11·88	14·50	21·35
			Titre	9·50	9·50	8·30	8·35	7·40	6·70	5·60
			% Reaction	0	2·13	5·31	12·21	22·35	29·80	41·50
	Pyridine	2·002	Time	0	1·72	6·43	13·52	17·13		
			Titre	9·60	9·40	8·60	7·20	6·60		
			% Reaction	0	2·08	10·42	25·00	31·25		

TABLE II. *Catalysed Reaction between Trans Crotonic Acid and Bromine*

Catalyst and Temp. °C.	Catalyst / Bromine moles %		Concentration of reactants : M/10						
IBr at 30°	9·874	Time	0	14·08	22·42	46·83	92·55	170	371
		Titre	10·10	9·40	9·10	8·00	6·90	5·70	4·40
		% Reaction	0	7·64	10·91	22·95	34·97	48·80	62·30
	5·014	Time	0	25·27	54·35	130	202	313	438
		Titre	9·50	9·10	8·60	7·45	6·60	5·60	5·00
		% Reaction	0	4·44	10·00	22·78	33·01	43·34	50·00
ICl at 30°	10·84	Time	0	209	1000	1580	1670	1769	1853
		Titre	9·50	9·20	8·90	8·20	7·50	6·81	6·10
		% Reaction	0	3·60	7·23	14·45	24·09	31·93	40·97
	5·142	Time	0	80·83	483	583	693	1000	1236
		Titre	9·25	9·10	7·65	6·90	6·25	5·35	4·55
		% Reaction	0	1·71	18·28	26·86	34·29	44·28	53·71
IBr at 35°	4·827	Time	0	1·07	12·77	151·5	1214	2594	
		Titre	10·15	10·10	9·90	9·05	8·00	7·05	
		% Reaction	0	0·52	2·58	11·34	22·16	32·47	
	1·922	Time	0	9·28	50·60	553	1223	4085	
		Titre	9·95	9·90	9·55	9·10	8·15	7·05	
		% Reaction	0	0·51	4·10	8·72	18·46	29·75	
	0·9506	Time	0	10·45	52·0	626	2760	40·94	
		Titre	9·95	9·90	9·60	8·80	7·45	7·00	
		% Reaction	0	0·51	3·05	11·68	25·39	29·95	

DISCUSSION OF RESULTS

In any catalysed reaction, the function of the catalyst is essentially to alter the activation energy of the reaction. This may be brought about by changes in the activation of either or both reactants. The first observable effect is the elimination of the induction period which is noticed in the present observations with all the catalysts studied (see Figs. 1 and 2). The behaviour of iodine chloride appears to be quite complex and after a fuller investigation will be communicated later. The insolubility of pyridine perbromide precluded a study of higher concentrations than the one reported. The trend, however, seems to be analogous to that of iodine bromide.

For a homogeneous reaction in which both reactants are activated by the catalyst, it has been shown earlier, that the rate equation can be represented by

$$\frac{dx}{d\epsilon} = k_2' [A] [Br_2] \frac{f}{f+1}$$

It has also been noticed that at higher temperatures, the rate equation reduces to a simple bimolecular one in acetic acid solutions. In the nonpolar solvent used in the present work, no constancy in the rate constant could be found as may be seen from the Figs. 3 and 4 showing the drift of the " bimolecular

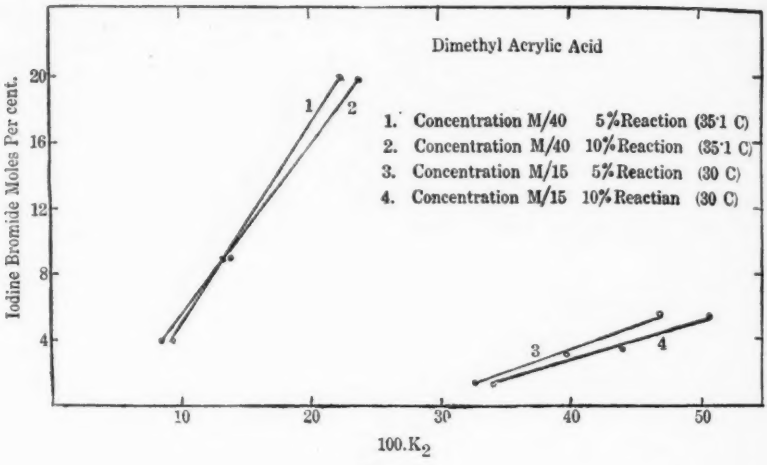

FIG. 3

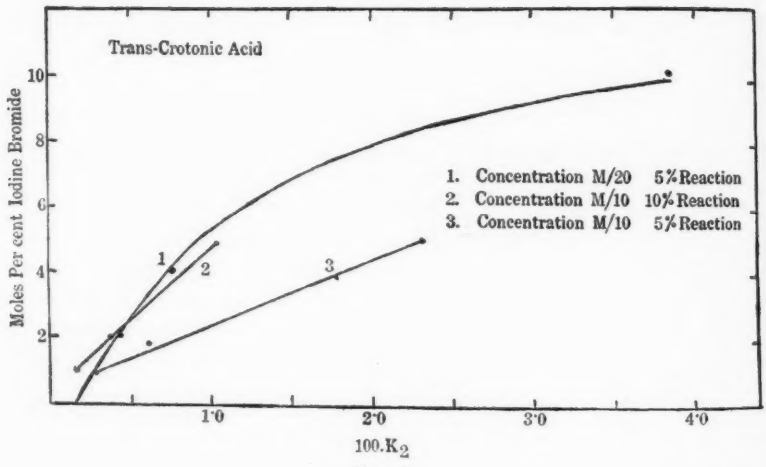

FIG. 4

rate constants " with the extent of reaction. The addition of the catalyst is not adequate for changing over to homogeneous conditions. This is well

rought out by a comparison of the time required for a given fraction of the reaction with reference to the catalyst concentration.

The catalysed reaction also brings out the pronounced influence of structure. Temperature does not seem to have any appreciable effect with dimethyl acrylic acid while it is quite noticeable with crotonic acid. This is in keeping with the observations in acetic acid solutions that the influence of catalysts on the dimethyl acrylic acid is small on account of the prior activation of the double bond by the two methyl groups on the same carbon atom.

One aspect of the catalysed reaction which has to be explained and which requires further study is the fact that initially the catalysed reaction is faster than the one with increased surface for the same initial concentration but the later stages are definitely slower. This is noticeable primarily with trans crotonic acid. Two possible causes of such slowing down are changes in frequency factor which is related to the shape of the olefine molecule and retardation by products of the reaction in a non-polar solvent. This is still under investigation.

Summary

Iodine bromide and chloride as well as pyridine have been used as catalysts for the reaction between bromine and crotonic and dimethyl acrylic acids. The reaction is quite complex and does not seem to conform to any simple rate equation. Even with the addition of the catalyst, the heterogeneous part of the reaction does not seem to be eliminated.

References

1. Anantakrishnan, S. V. and Venkatraman .. *Proc. Ind. Acad. Sci.*, 1946, **23A**, 306, etc.
2. Venkatraman, R. .. *Ibid.*, 1941, **13A**, 259.

NORTH-SOUTH ASYMMETRY OF COSMIC RAYS

By D. S. R. Murty

(From the Physical Laboratories, Osmania University, Hyderabad)

Originally received March 5, 1954

Received in revised form August 7, 1954
(Communicated by Prof. S. Bhagavantam)

1. Introduction

On the Lemaitre-Vallarta theory of the allowed cone (Montgomery, 1949) an asymmetry between the north and south unidirectional intensities is to be expected (Lemaitre and Vallarta, 1933; Lemaitre, Vallarta and Bouckaert, 1935). For positive particles the cone at the equator opens from the west and is symmetrical with respect to the east-west plane. As the latitude increases, the eastern boundary of the cone of a given energy moves towards the east and markedly shifts towards the south. As a result, in the northern hemisphere there is greater intensity from the south than from the north. For negative particles the cones are the mirror images, with respect to the meridian plane, of those for the positive particles. Therefore the southern effect will be the same for positive as for negative particles while the east-west effect will be reversed. Hence the north-south asymmetry depends on the sum of the positive and negative intensities while the east-west asymmetry depends on their difference (Lemaitre, Vallarta and Bouckaert, *loc. cit.*). In the southern hemisphere, the cones would be the mirror images, with respect to the east-west plane of those in the northern hemisphere and the southern excess observed in the northern hemisphere should be replaced by a northern excess, irrespective of the particles' sign. The north-south asymmetry depends for each latitude on a narrow band of energy. Irrespective of the particles' sign the energy region explored by this asymmetry varies considerably with latitude. Also the effect of the earth's shadow results in a large north-south asymmetry at high zenith angles for intermediate latitudes. For low latitudes, the asymmetry near the horizon should therefore be reduced (Lemaitre and Vallarta, 1936).

Johnson performed his experiments at Mexico ($\lambda = 29°$ N.) to study the north-south asymmetry at altitudes of 14,000 feet and 7,500 feet. A definite southern excess was found at most of the zenith angles at both stations. In his experiments the asymmetry reaches a minimum of 1·2 per cent. with a greater probable error at about 45° zenith angle at Nevado de

Toluca (alt. 14,000 feet). At 11,000 feet no asymmetry was observed at 45° zenith angle, while at Copilco (alt. 7,500 feet) the asymmetry at 32° zenith angle was nil. In fact the theory predicts a reversal of sign of asymmetry for zenith angles between 45° and 55° which depends upon the existence of a narrow energy band. A northern excess (2·9 per cent.) at Asmara, $\lambda = 11 \cdot 5°$ N. and altitude 2,370 m. at a zenith angle of 45° slightly larger than the rather large experimental error was reported by Rossi (1934). The experiments of Vallarta, Perusquia and De Oyarzabal (1947) at $\lambda = 29°$ N, $h = 2{,}240$ m. in connection with the studies of complete azimuthal effect show about 2 per cent. asymmetry at zenith angles 20° and 40° while at 60° the asymmetry disappears. Gill's (1945) experiments at Lahore ($\lambda = 22°$ N.) performed with a lead block filter for the azimuthal studies give an asymmetry slightly more than 7 per cent. at a zenith angle of 60°. The azimuthal study of Bhowmik and Bajwa (1952) with a lead block of 10 cm. thickness at Delhi, $\lambda = 19°$ N. yields more than 5 per cent. asymmetry at a zenith angle of 40°. Clay (1935) found a north excess at 10° and 20° zenith angles in Bandoeng ($\lambda = 18°$ S.). He reported about 4 per cent. asymmetry at 20° zenith angle. D. W. P. Burbury (1952) has got a value of $0 \cdot 0056 \pm \cdot 0013$ the excess being in the north for zenith angle 30° at sea level under 12 cm. of lead at a high geomagnetic latitude of 51·7° S. (Hobart, Tasmania). Bouckaert (1934) calculated north-south asymmetry for geomagnetic latitudes of 10° and 20° and moderate zenith angles.

A knowledge of both north-south and east-west asymmetries gives information on the ratio of positive to negative primaries (Vallarta, 1948; Janossy, 1950) in a given energy range (Vallarta, 1939). Also the penumbra hardly plays a part in the north-south effect unlike in the east-west effect. Experiments on the north-south asymmetry furnish the most direct approach to the study of energy spectrum. A complete and systematic experimental study of the north-south asymmetry was not reported except by Johnson (*loc. cit.*) whose investigations correspond to an intermediate latitude ($\lambda = 29°$ N.). The present work is undertaken at Hyderabad, India; $\lambda = 7 \cdot 7°$ N., the height above mean sea level being 1,800 feet.

2. Experiment

The cosmic ray telescope (Murty, 1953) used subtends an angle of 7° 2′ in the zenith and about 67·5° in the lateral plane, the distance of separation between the two extreme counters being 57 cm. The counters are 38 cm. long and 3·5 cm. in diameter. Observations were taken at several zenith angles. The telescope was oriented at a particular zenith angle in the northern azimuth and the counts were recorded. It was then rotated and

oriented at the same zenith angle in the south and the counts recorded. This process was repeated a number of times and the total number of counts from the north and south were obtained. The time of exposure of the telescope at each zenith angle each time is 15 minutes. The observations have been taken over a period of eight months. Readings were taken with 10° interval in all the cases except between 40° and 45° where the observational points are closely chosen in order to compare with Rossi's result at Asmara $\lambda = 11{\cdot}5°$ N. for $\theta = 45°$. Probable errors were calculated from the total number of counts (σ_c) and also computed from the residuals (σ_r).

No correction is made for the accidentals as the horizontal rate is about 3 per cent. of the vertical rate (Johnson, 1935). The asymmetry is given

TABLE I. *North-South Asymmetry of Cosmic Rays*

(Hyderabad, India; $\lambda = 7{\cdot}7°$ N. and altitude 1,800 ft.)

Zenith Angle θ		Time in minutes T	Total counts C	Counting rate $\frac{C}{T}$	Probable errors from		% Asymmetry $= 200\frac{I_s - I_n}{I_s + I_n}$	
					Total counts σ_c	Residuals σ_r	Experimental value at $\lambda = 7{\cdot}7°$ N.	Theoretical value at $\lambda = 10°$
10°	N ..	4590	12347	2·690	·016	·017	1·109 ± ·505	0·865
	S ..	4590	12487	2·720	·016	·016		
20°	N ..	3930	9254	2·355	·017	·018	2·433 ± ·523	1·875
	S ..	3930	9483	2·413	·017	·019		
30°	N ..	3930	7951	2·023	·015	·016	3·258 ± ·645	2·783
	S ..	3930	8216	2·090	·016	·016		
40°	N ..	4620	8058	1·746	·013	·014	2·768 ± ·452	3·033
	S ..	4620	8292	1·795	·013	·014		
45°	N ..	5790	8918	1·540	·011	·012	−1·439 ± ·452	3·303
	S ..	5790	8790	1·518	·011	·011		
55°	N ..	6150	6331	1·029	·009	·009	−0·683 ± ·435	3·356
	S ..	6150	6283	1·022	·009	·010		
65°	N ..	6150	4679	0·7607	·007	·008	2·544 ± ·645	3·956
	S ..	6150	4800	0·7803	·008	·009		
75°	N ..	6000	3232	0·5387	·006	·007	4·286 ± ·556	5·490
	S ..	6000	3375	0·5623	·007	·008		

as the ratio of the difference of intensities at the same zenith angle to their mean value, $\alpha = 2(I_s - I_n)/(I_s + I_n)$ where I_s and I_n are the counting rates from south and north respectively.

The results are given in Table I and plotted in Fig. 1. The theoretical north-south asymmetry values for geomagnetic latitude 10° are also given in Table I and plotted in Fig. 1. The asymmetry value obtained by Rossi for $\theta = 45°$ at Asmara can also be seen in the figure.

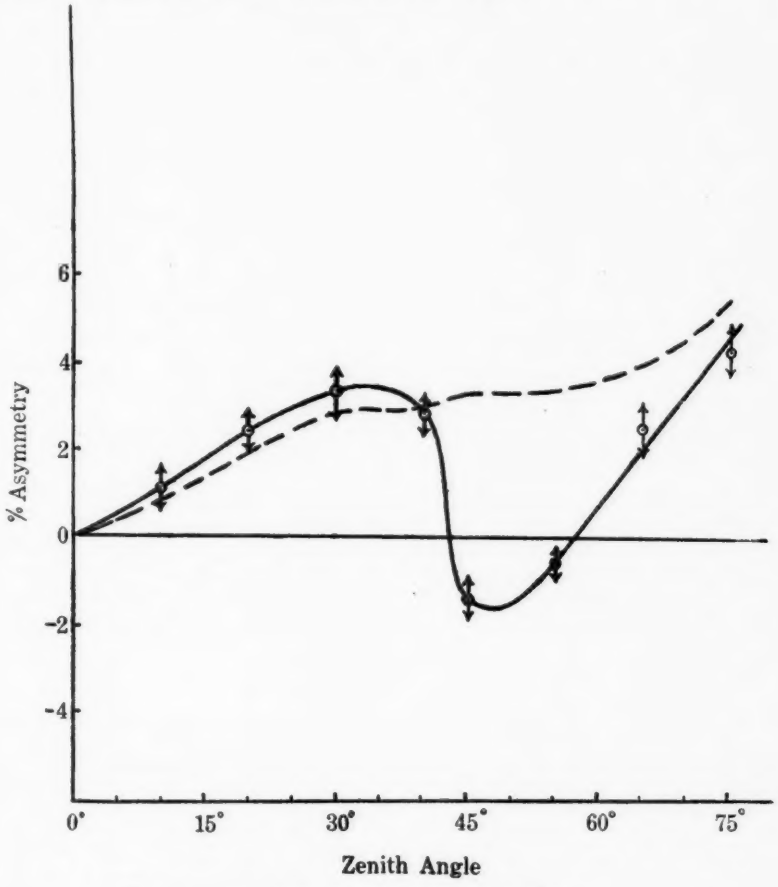

FIG. 1. North–South Asymmetry of Cosmic Rays

———— Experimental Curve at Hyderabad λ=7·7°N

- - - - - Theoretical Curve for λ=10°

⊗ Rossi's Observation Point at Asmara λ=11·5°N

3. RESULTS AND DISCUSSION

The results clearly show the southern excess of intensities at most of the zenith angles. The theory predicts a slight reversal of the sign of asymmetry for zenith angles between 45° and 55° which depends upon the existence of a narrow band of energy. This reversal begins at latitudes around 20° for zenith angles 70° and eventually broadens out so as to include the whole region between the zenith and 40° at latitudes around 35°. In the present case, at such a low geomagnetic latitude as 7·7° N., the reversal occurs at 45° and 55°. A negative asymmetry (2·9 per cent.) definitely greater than the rather large experimental error was already reported by Rossi (*loc. cit.*) at a geomagnetic latitude of 11·5° N. Even Johnson's experiments showed no asymmetry at 45° zenith angle at Mexico $\lambda = 29°$ N., $h = 11{,}000$ feet, and a low asymmetry less than the probable error at the same zenith angle at 14,000 feet. His experiments at Copilco ($\lambda = 29°$, $h = 7{,}500$ feet) yielded no asymmetry for a zenith angle of 32°. The reversal in the present case may be due to secondary effects due to absorption in the atmosphere or due to a narrow band of energies. The low value of the asymmetry at zenith angles near the horizon is quite in agreement with theoretical prediction based on the consideration of the shadow effect of the earth. The asymmetry near the zenith is explained by the theory of complicated orbits as developed by Lemaitre and Vallarta (*loc. cit.*). The agreement between the experimental curve and the theoretical curve for 10° is satisfactory except for the reversal at 45° and 55°. There is a striking similarity between this experimental curve and that got by Johnson's results at Mexico (14,000 feet). The differences in the values of asymmetry are due to differences in latitude and altitude.

The author offers his grateful thanks to Professor S. Bhagavantam for his helpful guidance and constant encouragement in the progress of the present work.

4. SUMMARY

The north-south asymmetry of cosmic rays is experimentally studied at Hyderabad, India; $\lambda = 7·7°$ N. and altitude 1,800 feet above mean sea level. A triple coincidence counter telescope with a resolution of 7° 2′ in the zenith and 67° 22′ in the lateral plane is employed. Observations are taken at several zenith angles. The results show the southern excess of intensities at most of the zenith angles. There is a reversal of the sign of asymmetry at zenith angles 45° and 55°, which is reported for the first time at such a low latitude of 7·7° N. The values of asymmetry near the zenith and the horizon are in general agreement with the theory.

REFERENCES

Bhowmik, B. and Bajwa, G. S. .. *Phys. Rev.*, 1952, **87**, 530.

Bouckært, L. . *Ann. Soc. Sci. Bruxelles*, 1934, A **54**, 174.

Burbury, D. W. P. .. *Phys. Rev.*, 1952, **86**, 577.

Clay, J. .. *Physica*, 1935, **2**, 861.

Gill, P. S. .. *Phys. Rev.*, 1945, **67**, 347.

Janossy, L. .. *Cosmic Rays*, Oxford University Press, 1950.

Johnson, T. H. .. *Phys. Rev.*, 1935, **47**, 91 & 326.

——— .. *Ibid.*, 1935, **48**, 287.

Lemaitre, G. and Vallarta, M. S. .. *Ibid.*, 1933, **43**, 87.

——— .. *Ibid.*, 1936, **49**, 719.

——— .. *Ibid.*, 1936, **50**, 493.

——— ,——— and Bouckært, L. .. *Ibid.*, 1935, **47**, 434.

Montgomery, D. J. X. .. *Cosmic Ray Physics*, Princeton University Press, 1949.

Murty, D. S. R. .. *Proc. Ind. Acad. Sci.*, 1953, **37**, 317.

Rossi, B. .. *Ricerca Scient*, 1934, **5**, 579.

Vallarta, M. S. .. *Frank. Inst. J.*, 1939, **227**, 1.

——— .. *Phys. Rev.*, 1948, **74**, 1837.

——— , Perusquia, M. L. and J. De Oyarzabal .. *Ibid.*, 1947, **71**, 393.

DIFFERENT OXIDATION STATES OF MANGANESE PRODUCED BY THE Fe(n, p)Mn REACTION

By C. Lakshman Rao, Hari D. Sharma and Jagdish Shankar
(*Atomic Energy Commission Chemistry Laboratory, Bombay*)

Received June 10, 1954
(Communicated by Dr. H. J. Bhabha)

Alper and Preez[1] noted that Mn^{54} is formed by the $Fe^{54}(n, p)Mn^{54}$ reaction but Frierson and Jones[2] reported its absence in irradiated iron. Michalowicz and Lederer[3] using chromatographic methods of separation also failed to observe any Mn^{54} activity in irradiated iron. While our work was in progress Stafford and Stein[4] published their results supporting the observations of Alper and Preez. The present investigations confirm the formation of Mn^{54} as a result of (n, p) reaction in Fe^{54}.

Various workers[5-9] have observed that the products of (n, p) reactions often exist in different oxidation states. It was therefore decided to study the different oxidation states of Mn^{54} produced from Fe^{54}.

Ferric oxide prepared from carefully purified E. Merck's G.R. quality ferric chloride, was irradiated with fast neutrons at Atomic Energy Research Establishment, Harwell. Spectroscopic analysis of Fe_2O_3 showed that it was of a high degree of purity and that cobalt was completely absent.

To extract any manganese activity in the form of manganous ions, about 0·5 g. of irradiated ferric oxide was treated with a solution of $MnCl_2$ at 100° C. for 6 hours with intermittent stirring. Fe_2O_3 was centrifuged out, the solution filtered through Whatman No. 42 and MnO_2 was precipitated in the filtrate with potassium bromate in 2 N nitric acid solution. The precipitate was centrifuged, washed, dissolved in nitric acid and reprecipitated as above. The cycle of operation was repeated five times. For extracting MnO_4^- ions, ferric oxide was treated with potassium permanganate solution at 100° C. for six hours and after removal of Fe_2O_3, MnO_2 was precipitated by adding concentrated hydrochloric acid. It was purified as in the previous case. In both cases iron and chromium solutions were added as holdback carriers.

For determination of the total manganese activity 0·5 g. of ferric oxide was dissolved in hydrochloric acid, manganese and chromium were added as carriers, the solution made to 6 N in hydrochloric acid and iron was

extracted with ether. In the aqueous phase manganese was precipitated and purified as described above. The decay curve of the separated fraction shown in Fig. 1 showed that the 320-day activity of Mn^{54} was quite pure.[10]

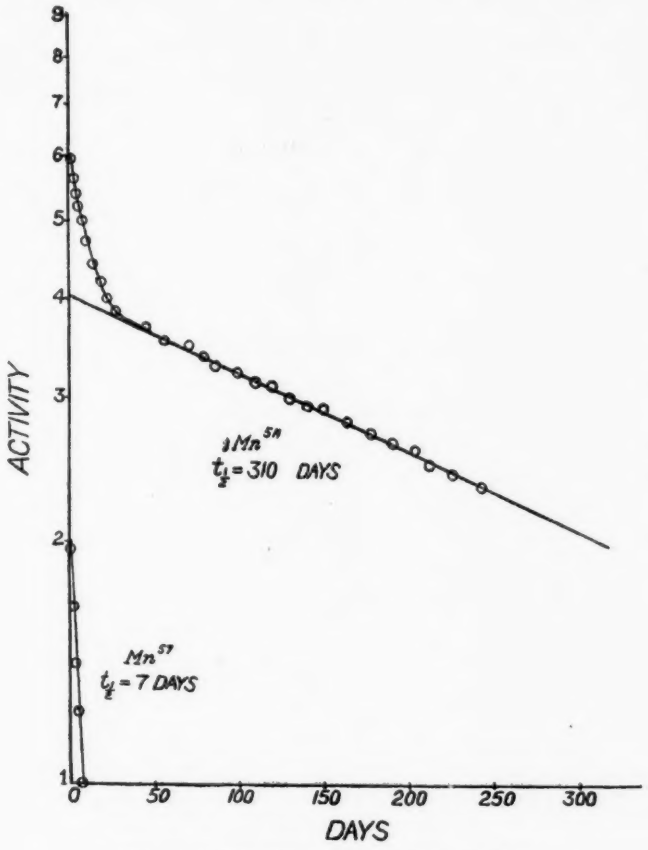

FIG. 1, Decay Curve of Manganese Fraction

To further confirm the formation of Mn^{54}, some of this active MnO_2 was dissolved in hydrochloric acid, some Co^{60} and Fe^{59} added and a drop of the resulting mixture chromatographed according to the methods described by Michalowicz and Lederer[3] and Burstall *et al.*[11] Unequivocal proof of the presence of Mn^{54} was obtained by this method.

Isotopic exchange of MnO_2 with $MnCl_2$ and $KMnO_4$ solutions was studied by Polissar[12] at ordinary temperatures and by the authors at 100° C.

No exchange whatsoever was observed. In the extraction of manganese activity with $MnCl_2$ and $KMnO_4$, weighed amount of irradiated ferric oxide was treated with successive amounts of the respective solutions till the extract showed no activity. Several determinations gave the following mean results:

Extraction with $KMnO_4$ at pH 9	..	274 ± 30 cpm.
Extraction with $MnCl_2$ at pH 5	..	327 ± 30 cpm.
Total Manganese	..	13,350 ± 100 cpm.

Whereas all Mn^{++} was completely extracted out with $MnCl_2$ is about 3 extractions, MnO_4^- required about 6 extractions with $KMnO_4$. In the case of potassium permanganate, it was noticed that the separable activity at pH 2·5 was greater than that at pH 12.

DISCUSSION

The results obtained in the present investigations leaves no doubt that Mn^{54} is formed as a result of the (n, p) reaction in Fe^{54} thus confirming the recent observations of Stafford and Stein.[4] Further it is found that some manganese is present in manganous and permanganate states but principally it is present as manganese dioxide.

In the (n, p) reaction the nuclear charge is reduced by one unit and hence iron in the trivalent state in such a reaction, one would essentially obtain manganese in bivalent state if no additional ionization occurs in an atom undergoing such a transformation. The formation of higher oxidation states as obtained in our experiments can be due to several complex and competing factors which are hardly understood for the present as pointed out by Burgus and Kennedy.[13] Some of them are as follows:—

(1) Passage of proton through the electronic shells.

(2) Production of daughter atom in an excited state which decays by γ-emission which may in turn be internally converted.

(3) Dissipation of recoil energy imparted to daughter nuclei (of the order of 100 KeV in this case).

(4) Secondary reactions of the recoil fragments with neighbouring molecules.

Michalowicz and Lederer[3] did not find manganese in irradiated iron perhaps because the amount of manganese in the solution chromatographed was very small. Since in the present work Mn^{54} was concentrated in the MnO_2 fraction used for chromatography, a clear zone of manganese was obtained.

SUMMARY

Formation of Mn^{54} by (*n*, *p*) reaction in Fe^{54} has been confirmed. It has been found that Mn^{54} thus formed occurs in the several oxidation states.

REFERENCES

1. Alper, T. and du Preez, L. .. *Nature*, 1950, **165**, 689.
2. Frierson, W. J. and Jones, W. .. *Anal. Chem.*, 1951, **23**, 1447.
3. Michalowicz, A. and Lederer, M. .. *J. de Phys. et le. Radium*, 1952, **13**, 669.
4. Stafford, G. H. and Stein, L. H. .. *Nature*, 1953, **172**, 1103.
5. Aten, A. Jr. .. *Phys. Rev.*, 1947, **71**, 641.
6. Edward, R. R. *et al.* .. *J. Amer. Chem. Soc.*, 1948, **70**, 1670.
7. Kamen, M. D. .. *Phys. Rev.*, 1941, **60**, 537.
8. Ruben, S. and Kamen, M. D. .. *Ibid.*, 1941, **59**, 349.
9. Yankwich, P. E., Rollefson, G. K. and Norris, T. H. *J. Chem. Phys.*, 1946, **14**, 131.
10. Livingwood, J. J. and Seaborg, G. T. *Phys. Rev.*, 1938, **54**, 391.
11. Burstall, F. H. *et al.* .. *J. Chem. Soc.*, 1950, 516.
12. Polissar, M. J. .. *J. Amer. Chem. Soc.*, 1936, **58**, 1372.
13. Burgus, W. H. and Kennedy, J. W. .. *J. Chem. Phys.*, 1950, **18**, 97.

1184-54 Printed at The Bangalore Press, Bangalore City, by C. Vasudeva Rao, Superintendent and Published by The Indian Academy of Sciences, Bangalore

NOTICE TO AUTHORS

Scientific papers intended for publication in the *Proceedings of the Indian Academy of Sciences* can be accepted only when they are communicated by a Fellow of the Academy whose duty shall be to satisfy himself that such communications are fit to be read at the Meeting of the Academy and published in its *Proceedings*.

Papers should not ordinarily exceed fifty pages of foolscap. MSS. should be either typewritten or written in legible hand on one side of the paper. All papers should be carefully revised by the authors and should be absolutely in final form for printing. Position for text-figures should be indicated. Each paper shall conclude with a critical summary not exceeding 350 words.

Drawings, diagrams or other illustrations should be made on larger scale (preferably) twice the size than the ones in which they are intended to appear. They should be done in Indian ink on bristol board with lettering in pencil. Scale of magnification of camera lucida tracings should be indicated by the side of drawings. In certain special cases arrangements will also be made for monochrome lithographic and other colour plates. Reduction of illustrations desired should be indicated in pencil. Appropriate legends should accompany all drawings. Names of authors are to be marked in pencil on the left-hand corner of drawing sheets. Photomicrographs should be securely mounted with colourless paste.

All tables, quotations and footnotes which will be set hereafter (beginning from Vol. I, No. 2) in types smaller than the text, should be typewritten on separate sheets and placed with the text in proper sequence. Footnotes should be numbered in Arabic numerals.

References to literature in the text should be given, whenever possible, in chronological order, only the names of authors and years of publication, in brackets, being given. They should be cited in full after the summary, the authors' names following in alphabetical order. Thus,

Name or Names of author; Name of Journal (abbreviation) with a single underline; Year of publication; Number of Volume with a double underline, and lastly page. The following would be a useful illustration:—

Bergmann and Stather . . . . . Z. Physiol. Chem., 1926, 152, 189.

Two copies of slip-proof and wherever possible, a page proof for final revision will be sent to authors. All corrections are best made on the slip-proof which should be transmitted to the Office of the Academy. All proof corrections involve heavy expenses which would be negligible if the papers are carefully revised by the authors before submission.

Authors will be supplied with reprints of their papers at cost price, if intimation is given at the time of returning the slip-proof.

Blocks appearing in the *Proceedings* will be available for purchase by their respective authors. Orders for the same should be sent along with the corrected proofs and in any case not later than one month after the date of publication of the paper. The price charged would be 25% of the actual cost of the blocks *plus* freight and despatching charges. If the blocks are reproduced in other journals or publications, due acknowledgment should be made in them to the *Proceedings*.

The original drawings and plates of blocks appearing in the *Proceedings* will be returned to such of the authors as may require them provided the cost of despatching such originals is borne by them.

CONTENTS

PAGE

X-Ray Studies on Polycrystalline Gypsum . . . . . Sir C. V. Raman and A. Jayaraman 57

Angular Distribution of Protons Emitted in the Reaction $_7N^{14}(\alpha, p)_8O^{17}$ . . . . . G. S. Mani and R. Pandhi 61

An X-Ray Study of Natural Monazite: I . . . . . M. D. Karkhanavala and J. Shankar 67

Prominence Activity (1905–1952) . . . . . R. Ananthakrishnan 72

Kinetics of the Olefine-Bromine Reaction. Part VIII. The Catalysed Reaction between Bromine and Crotonic and Dimethylacrylic Acids in Carbon Tetrachloride Solutions . . I. M. Mathai and S. V. Anantakrishnan 91

North-South Asymmetry of Cosmic Rays . . . . . D. S. R. Murty 96

Different Oxidation States of Manganese Produced by the Fe(n,p) Mn Reaction . . . . . C. Lakshman Rao, Hari D. Sharma and Jagdish Shankar 102